The FASEB Journal

FASEB
Federation of American Societies for Experimental Biology

RESEARCH ARTICLE OPEN ACCESS

Surrogate GPR139 Agonists Reverse Short-Term Startle Habituation Impairment in Larval Zebrafish

Teck Fong Kow[1] | Siew Ying Mok[2] | Pek Yee Tang[2] | Lor Huai Chong[3] | Satoshi Ogawa[1]

[1]Jeffrey Cheah School of Medicine and Health Sciences, Monash University Malaysia, Bandar Sunway, Selangor Darul Ehsan, Malaysia | [2]Department of Mechatronics and Biomedical Engineering, Universiti Tunku Abdul Rahman, Kajang, Selangor, Malaysia | [3]School of Pharmacy, Monash University Malaysia, Bandar Sunway, Selangor Darul Ehsan, Malaysia

Correspondence: Satoshi Ogawa (satoshi.ogawa@monash.edu)

Received: 26 February 2025 | **Revised:** 5 May 2025 | **Accepted:** 9 May 2025

Funding: This work was supported by Monash Malaysia | Jeffrey Cheah School of Medicine and Health Sciences, Monash University Malaysia (JCSMHS), I-M010-STG-000225, I-M010-SED-000218.

ABSTRACT

GPR139, an orphan G-protein coupled receptor predominantly expressed in the habenula, has recently been implicated in understanding neurobehavior and neuropsychiatric disorders. Surrogate agonists for human GPR139 have shown the potential to alleviate cognitive impairment associated with schizophrenia in rodent models and human clinical trials. Yet, the effect of GPR139 agonists on the neurophysiological properties of the habenula remains elusive. We examined the effect of GPR139 agonists (JNJ-63533054 and TAK-041) on short-term startle habituation of 6-day post-fertilization (dpf) larval zebrafish (*Danio rerio*) in an automated solenoid setup and on reversing the pharmacologically impaired startle habituation. GPR139 agonists enhanced startle habituation at the lowest tested concentrations, whereas moderate and highest concentrations delayed startle habituation. Furthermore, GPR139 agonists reversed the non-competitive N-methyl-d-aspartate (NMDA) receptor antagonist MK-801-induced startle habituation impairment. Using exponential decay curve fit analysis, we found that the lowest concentration of GPR139 agonists performed better than moderate and highest concentrations in reversing the MK-801-induced impairment of startle habituation. Using in vivo GCaMP calcium imaging and phosphorylated extracellular-signal-regulated kinase (pERK) as a proxy for neural activity, we found that GPR139 agonists exerted effects on the habenula activities at the habituated state but not during the spontaneous state (without startle habituation paradigm), suggesting the GPR139 agonists-evoked neural activation in the habenula is sensory stimuli-dependent. Moreover, both GPR139 agonists differently reduced MK-801-induced hyperexcitability of the habenula at both spontaneous and habituated states. Taken together, we showed that GPR139 agonists reverse startle habituation impairment caused by MK-801 via the normalization of hyperexcitability of zebrafish habenula.

1 | Introduction

Cognitive impairments, including difficulties with attention, learning, and memory, are highly prevalent in schizophrenia, often preceding positive (e.g., hallucination) and negative symptoms (social withdrawal; [1, 2]) and present in 80% of patients [3]. Current antipsychotic drugs, mainly targeting the dopamine D_2 and serotonin 5-HT_{2A} receptors and affecting the dysfunctional frontal lobe [4, 5], are insufficient due to the complex pathophysiological mechanisms involving dopamine, serotonin, and imbalanced glutamatergic and GABAergic signals [6].

The habenula, a highly conserved bilateral nucleus, is divided into lateral (LHb) and medial (MHb) subdivisions in mammals [7]. LHb projects to the dopaminergic ventral tegmental area (VTA) [8, 9], and the serotonergic dorsal raphe nucleus [10, 11]. The habenula regulates aversive learning, emotional decision-making, sleep rhythmicity, and startle habituation [7, 12–16].

Schizophrenia patients have been reported to have dysfunctional habenula, which fails to regulate dopamine systems [17–21]. Examples of cognitive Impairment in schizophrenia (CIAS), such as startle response and sensorimotor gating, are affected by abnormal LHb that dysregulates the dopamine and serotonin systems [22–24]. However, understanding the role of the habenula in the pathophysiology of schizophrenia is still limited by the complexity of its functions, the heterogeneity of schizophrenia symptoms, the limitations of animal models, neuroimaging techniques, and the elusive molecular mechanisms involved.

The habenula is enriched with orphan G-protein coupled receptors (GPR) [25]. Among the orphan GPRs, a genetic-linkage twin study associated the *GPR139* with ADHD and schizophrenia [26, 27]. *GPR139* is highly conserved from fish to humans [28] and is associated with negative and cognitive symptoms in animal models of schizophrenia [29, 30].

In mammals, GPR139 is primarily expressed in the MHb and sparsely expressed in other areas such as the LHb, striatum, hippocampus, and VTA [31–33]. Contrastingly, in zebrafish, *gpr139* was exclusively expressed in the ventral habenula, homologous to the mammalian LHb [34]. While endogenous ligands for GPR139 remain debatable [35–40], several surrogate GPR139 agonists have been reported [35, 37, 41]. JNJ-63533054 has shown favorable potency profiles in vitro and in vivo assays [35, 38]. In rodents, GPR139 agonists improved deficits in alcohol dependence, mood dysregulation, reduced non-rapid eye movement (NREM) latency, and increased NREM sleep [42, 43]. We previously demonstrated that JNJ-63533054 blocked the consolidation of contextual fear memory in zebrafish [34]. Another GPR139 agonist, TAK-041, has shown therapeutic potential for schizophrenia symptoms in rat and human clinical trials [44, 45]. However, the neurophysiological role of GPR139 signaling in the habenula and its pathophysiological implications in neuropsychiatric disorders remain unknown.

In this study, we first examined the effect of activation of GPR139 signaling on startle habituation using GPR139 agonists (JNJ-63533054 and TAK-041) in larval zebrafish. We then assessed their impact on MK-801-induced impairment of startle habituation. Zebrafish is an ideal model for studying the neurophysiological role of GPR139 in the habenula due to their exclusive expression in the ventral habenula [34]. We first explored the effect of GPR139 agonists at various concentrations on behavioral performance, such as locomotion and startle habituation. Using in vivo calcium imaging and pERK immunohistochemistry, we next investigated the effect of GPR139 signaling activation on the habenula at a stimulation-free spontaneous state, followed by a habituated state. We found that treatment with GPR139 agonists facilitates startle habituation and reverses the MK-801-induced startle habituation impairment through the normalization of hypofunction of zebrafish habenula.

2 | Materials and Methods

2.1 | Fish Husbandry

Wildtype (WT) and transgenic *Tg*(*HuC:Gal4-VP16;UAS:GCaMP6s*) larval zebrafish (*Danio rerio*) at the age of 6 days post-fertilization (dpf) were used for the experiments. Larval zebrafish at 6 dpf were commonly used across behavioral and calcium imaging studies. We followed this standard practice to ensure comparability across studies. Larvae at 6 dpf could display robust cognition and behavior and had an unsealed blood–brain barrier that allowed compounds to reach brain regions via gill absorption. The transgenic larvae were obtained from the cross-breeding between *Tg*(*HuC:GCaMP6s*) and *Tg*(*UAS:Gal4-VP16*) parents, and the expression of GCaMP was confirmed at 3 dpf. For transgenic zebrafish larvae, the embryos were collected following standard protocols and raised in E3 medium (5 mM NaCl, 0.17 mM KCl, 0.33 mM $CaCl_2$, 0.33 mM $MgSO_4$, pH 7.2) and treated with 0.003% 1-phenyl 2-thiourea (PTU) before 12 h post-fertilization (hpf) until 6 dpf to avoid skin pigmentation. Larvae had yet to undergo sexual differentiation. Therefore, no male or female fish samples were specified. The fish were maintained at 28.5°C with a standard 10:14 LD cycle with the light switched on at 8 am. Larvae were fed from 5 dpf onwards with paramecium. Larvae were randomly selected for the experiment. Posterior power analysis showed sufficient strength in the sample size used.

This study was carried out in strict accordance with the recommendations in the guidelines to promote the well-being of animals used for scientific purposes: The assessment and alleviation of pain and distress in research animals (2008) by the National Health and Medical Research Council of Australia (https://www.nhmrc.gov.au/guidelines-publications/ea18). All experimental protocols and procedures were approved by the Animal Ethics Committee of Monash University Malaysia (project approval number: 2022-32635-79633).

2.2 | Compound Treatments

Surrogate GPR139 agonists, JNJ-63533054 (formally designated as compound 7c) and TAK-041 (also known as Zelatriazin or NBI-1065846) were purchased from Axon Medchem BV, Groningen, Netherlands. GPR139 agonists were dissolved in 100% DMSO and further diluted to 0.1% DMSO with E3 medium, which has been demonstrated to be a non-toxic dose [46], before being administered to larval zebrafish.

Various concentrations of GPR139 agonists were used (JNJ-63533054: 1.6 μM, 20 μM and 50 μM; TAK-041: 2.2 μM, 20 μM and 50 μM). The half-maximal concentrations (EC50) value of JNJ-63533054 on human GPR139 is comparable to that of zebrafish GPR139 and acts as an agonist on zebrafish [34]. In addition, TAK-041 is an analog of JNJ-63533054, and they largely share binding sites [40]. Hence, we used the EC50 value of human GPR139 as a reference to form the lowest concentration of both agonists [34, 35, 37, 41]. The moderate and high concentrations of compounds were selected to cover a broad concentration range, ensuring efficiency in testing, and were based on previous studies involving acute exposure for modulating the cognitive function of larval zebrafish [47, 48]. The control group was treated with either 0.1% DMSO or 100 μM MK-801.

To elucidate the effect of GPR139 on cognitive impairment, we used MK-801-induced cognitive impairment, which has been known as a model of CIAS in animal studies [48, 49]. Briefly, larval fish were exposed to 100 μM of MK-801 for 30 min prior

to the habituation assay. All drug treatments and experiments were conducted between 11 a.m. and 4 p.m. Experimenters were not blinded to the experimental condition.

2.3 | Assessing Compounds Effect on Locomotion

The effect of GPR139 agonists in larval zebrafish on locomotor activity was assessed ($n = 20$ for the treated groups and $n = 30$ for the control group). The 6 dpf WT larval zebrafish were individually placed in a 96-well plate with 300 μL of E3 medium in each well for sufficient locomotion space [50]. Immediately after administering the compounds, larvae were transferred into the observation chamber (DanioVision, Noldus, Wageningen, Netherlands) and recorded locomotor activity for an hour at 30 frames per second (fps). The experiment was conducted under the infrared light condition at 28°C as larvae free swimming was more consistent and more responsive to startle stimuli [51–53]. Various parameters, such as distance traveled, velocity (mm/s), and turn angle, which were built in EthoVision XT 15 software (Noldus, RRID:SCR_000441), were extracted.

2.4 | Apparatus and Analysis for Startle Habituation Paradigm

Startle habituation is a form of non-associative learning in which the impairment of this behavior is commonly assessed as a model of cognitive impairment associated with schizophrenia [54–58]. An apparatus to assess the startle habituation and sensorimotor gating in larval zebrafish was fabricated based on our previous study with a slight modification [59]. Briefly, an automated push-and-pull solenoid (element14, Singapore) adhered to the center of the wall of a 24-well plate (Figure 2A) to provide mechanical tapping as vibrational stimuli. Larvae were individually placed in the 24-well containing a final amount of 500 μL of the compound and E3 medium ($n = 24$ for the treated groups and $n = 32$ for the control group). The paradigm consisted of 3 blocks of 30 trials of startle stimuli with a 1-s interstimulus interval (ISI). The solenoid was programmed by Arduino IDE. The experiment was conducted in the observation chamber (DanioVision).

The startle response was measured using built-in parameters–mobility state–of EthoVision XT 15 (Noldus, RRID:SCR_000441), which measures the percentage of change in the surface area of larvae between frames of recording. The average sample was set to 1. The percentage of change was fixed at 30%, meaning a displacement of 30% of the larvae body area was considered a startle response. The response was binned in 1 s. A startle response was quantified with a value 1, whereas a non-startle response was quantified with a value 0. The probability of startle response for each trial was the average of the startle responses of all larvae in the group. Larvae that failed to respond to the first startle stimuli were excluded from the analysis. All included data was analyzed, and no data was lost.

Moreover, to examine the characteristics of startle habituation [57], an exponential decay curve analysis was conducted. The first-order exponential decay curve was fitted to the probability of startle response for each group and block, generating three parameters: amplitude, plateau, and tau values. The decay curve was fitted using the least square regression model on Prism 10 (GraphPad) (RRID:SCR_002798). The built-in equation of the decay curve was: $Y = (Y_1 - P) * \exp^{(-K*X)} + P$, where Y stands for the probability of startle response at a certain trial, Y_1 stands for amplitude as the probability of response in the first trial; P stands for plateau as the habituated probability of response; K is rate constant with a unit of reciprocal of the number of trials $\left(\frac{1}{X}\right)$; and X stands for a trial number. Amplitude (Y_1), plateau (P), and tau ($\frac{1}{K}$) parameters of the exponential curve were extracted after 1000 iterations with varying probabilities of response within the standard deviation. Tau was defined as the number of trials required for the first trial startle response to fall below 37% of the response, which determines the rate of habituation. Parameters were based on reference [60, 61]. These parameters reflected the characteristics of startle habituation. For instance, decreasing amplitude across blocks of trials indicated a reduction in startle magnitude and spontaneous recovery; decreasing tau across blocks of trials indicated potentiation of habituation; decreasing plateau across blocks of trials indicated habituation beyond asymptotic response level. To extract each parameter without interference from other parameters, different Y_1, P, and K criteria were constrained to obtain amplitude, plateau, and tau. Amplitude was extracted from the fitting analysis with criteria of $Y_1 < 1$, $p > 0$ and $K > \frac{1}{30}$. Plateau was extracted with criteria of $Y_1 = 1$ and $K > \frac{1}{30}$. Tau was extracted with the criteria of $Y_1 = 1$, $p = 1$ and $K > \frac{1}{30}$.

Larvae were acclimated for at least an hour on the 24-well plate before the administration of the compounds. Larvae were exposed to the GPR139 agonists for 30 min before the trial. Data were extracted using a customized MATLAB (RRID:SCR_001622) (Mathworks, USA) script. Only larvae that were responsive to the first trial met the inclusion criteria.

2.5 | MK-801-Induced Startle Habituation Impairment

MK-801 is a common NMDA receptor antagonist that modeled cognitive impairment similar to schizophrenia phenotypes. 100 μM of MK-801 was used based on the reference of past studies on larval zebrafish [47, 48]. To test the effect of GPR139 agonists on MK-801-induced habituation impairment, larvae were first exposed for 30 min to 100 μM MK-801, followed by the administration of the GPR139 agonist to the medium with MK-801 for another 30 min ($n = 24$ for all groups). The solutions containing MK-801 and GPR139 compounds were present throughout the experiment to avoid the wash-out.

2.6 | Spontaneous Neural Activity of Larval Zebrafish Habenula

To measure the effect of GPR139 agonists on habenula cells signaling, we measured the spontaneous activity of habenula cells with different compound exposures in Tg(HuC:Gal4-VP16;UAS:GCaMP6s) larval fish. Based on the behavioral experiment, the lowest concentration of GPR139 agonists showed more consistent facilitation on startle habituation. Hence, we chose the

lowest concentrations of both agonists for the subsequent experiment. The effect of the lowest concentration GPR139 agonists (1.6 μM of JNJ-63533054 and 2.2 μM of TAK-041) on spontaneous neural activity of the whole habenula was recorded ($n = 6$ for the treated and the control groups, except group cotreated with MK-801 and JNJ-63533054, MKJNJ-treated group, is $n = 7$). Larva was individually mounted on 2% low melting point agarose (Sigma-Aldrich, USA), submerged in E3 medium in a 35 mm glass-bottom petri dish, and given sufficient time to acclimate. Larva was subjected to a selected compound for 20 min on the microscope stage in the dark condition at 25°C, followed by 10 min of recording to measure any change in the neural activity (either the effect had taken place or gradually accumulating) before the behavioral role was evident. We consistently recorded a single plane at the z position in which the midsection of the habenula commissure is visible, where both ventral and dorsal habenula subnuclei are clearly visible, as identified based on the atlas on https://www.mapZebrain.org [62, 63]. Leica SP8 MP confocal imaging (Leica, Germany) and water-immersion 25× objective lens (HC FLUOTAR L 25×/0.95 WATER) were used. Resonant scanning and bidirectional X scanning were switched on to achieve 14.62 frames per second (fps) and 36 ns (ns) pixel dwell time when scanning 1024 × 256 pixels. 10% laser power, 1.6× zoom, 1.0 pinhole, and line averaging were applied. Laser frequency 488 nm was used to image GCaMP6s.

Confocal recording image sequences were stacked using Fiji software (RRID:SCR_002285) [64], followed by background subtraction and Gaussian blur with 1 sigma radius to improve neural activity detection. Raw fluorescence was extracted using suite2p software (RRID:SCR_016434) [65]. $\Delta F/F_0$ was calculated by subtraction of raw fluorescence (F) with baseline fluorescence (F_0) and divided by baseline fluorescence: $\Delta F / F_0 = (F - F_0) / F_0$. F_0 for each second was the minimum value of the 3 s window centred at that second of the 20% quartile of raw fluorescence neural activities, followed by a smoothed curve fit. Frequency of firing was collected for signals higher than two standard deviations of mean $\Delta F/F_0$ for each recording [66]. Average activity was calculated by finding the area under the curve via the MATLAB (RRID:SCR_001622) *trapz()* function [67]. Only larvae that remained active after imaging met the inclusion criteria for data analysis. All included data was analyzed, and no data was lost.

2.7 | Phosphorylated Extracellular Signal-Related Kinase (pERK) Immunohistochemistry

The effect of GPR139 agonists on the habenula during the startle habituation was examined using the phosphorylated ERK (pERK) immunostaining protocol ([68], STAR Protocols: https://doi.org/10.1016/j.xpro.2022.101731). The WT larval fish were collected before and after the startle habituation with or without GPR139 agonists and MK-801 (see above), and the whole larval were subjected to immunofluorescence for monoclonal mouse Anti-p44/42 MAP Kinase (Cell Signaling Technology, Cat# 4696; RRID: AB_390780; Dilution 1:500) for total ERK (tERK) and monoclonal rabbit Anti-Phospho p44/42 MAP Kinase (Thr202/Tyr204) for pERK (Cell Signaling Technology, Cat# 4370: RRID: AB_2315112, Dilution 1:500) followed by incubation with Anti-mouse IgG conjugated with Alexa Fluor 594 (Thermo Fisher Scientific, RRID: AB_2534095) and Anti-rabbit IgG conjugated with Alexa Fluor 488 (Thermo Fisher Scientific, RRID: AB_2534069), respectively. Planes of tERK and pERK immunofluorescence were observed and captured under a laser confocal microscope (SP8 MP, Leica, Germany) with 488 nm and 552 nm lasers, respectively. For each subject, three 1 μm (μm) planes were captured, and each plane was 7 μm Z-depth apart. The first plane of each subject was always the plane where the commissure was visible. Each plane was either Look Up Table (LUT) inverted (for tERK image) or not (for pERK image) before the signal improvement procedure, such as background subtraction, smoothing, Gaussian blur, and enhanced contrast, followed by local maxima to identify post hoc neural firing. Contour detection was further improved by eroding and watershed processing before measuring neural firing intensity. The captured confocal images were analyzed using a self-written script in Fiji software (RRID:SCR_002285). The pERK over tERK ratio was calculated for each plane (pERK/tERK value = $pERK / tERK$) and analyzed using a self-written MATLAB (RRID:SCR_001622) script. Due to technical difficulties, 2 larvae were lost for each treated group and the control group (final $n = 4$), except the JNJ-treated group lost 1 larva (final $n = 5$) and no sample loss for the TAK-treated group (final $n = 6$).

2.8 | Statistical Tests

The analysis was performed using Prism 10 (GraphPad, RRID:SCR_002798). For spontaneous swimming analysis, the Kruskal–Wallis test was used to compare the GPR139 groups, followed by Dunn's multiple comparison tests to compare the control with each concentration of GPR139 groups. For the startle habituation paradigm, the Mann–Whitney test and Kruskal–Wallis tests, followed by Dunn's multiple comparison tests, were used accordingly. For spontaneous activity analysis, the Wilcoxon test, Friedman test, and Kruskal–Wallis test, followed by Dunn's multiple comparisons tests, were used accordingly. A significant difference in statistical tests was observed at $p < 0.05$.

2.9 | Code Accessibility

Self-written scripts for quantification of habenula cells spontaneous activity and activation intensity via pERK immunohistochemistry are available on the GitHub repository: https://github.com/davidkow9999/GPR139_IVCL_Scripts.git.

3 | Results

3.1 | Locomotion Effect of GPR139 Agonists

We first examined the locomotion effect of the GPR139 agonists (JNJ-63533054 and TAK-041, referred to as JNJ and TAK, respectively, in the following sections) in larval zebrafish. There was no difference in all parameters examined–distance travel, turn angle, and velocity–between the control and JNJ group (distance travel: $H = 2.404$, $p = 0.493$; turn angle: $H = 2.412$, $p = 0.491$; and velocity: $H = 2.473$, $p = 0.480$, Figure 1A–C) and between the control and TAK group (distance travel: $H = 2.011$, $p = 0.570$; turn angle: $H = 6.619$, $p = 0.085$; and velocity: $H = 2.042$, $p = 0.564$, Figure 1D–F).

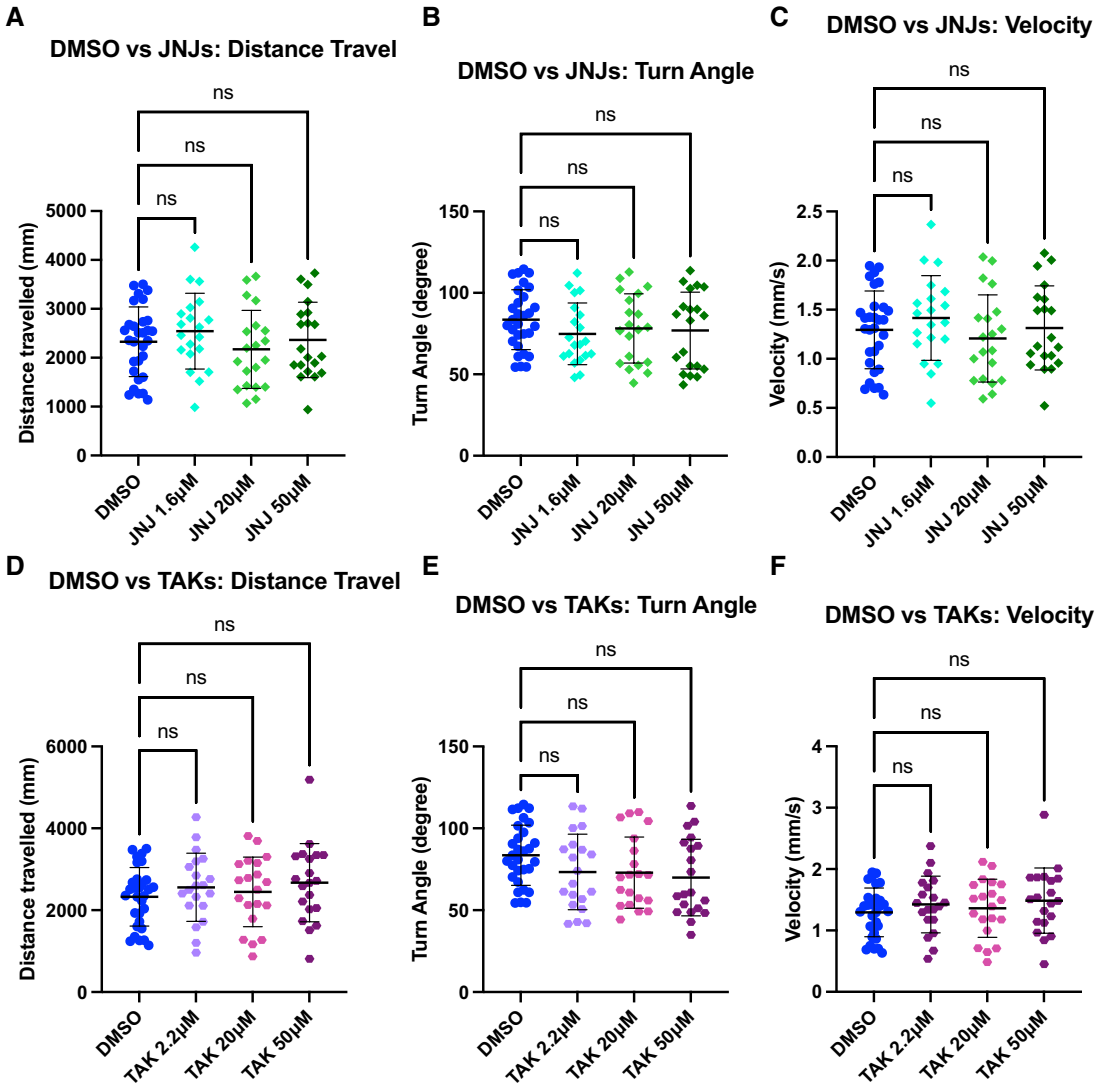

FIGURE 1 | Spontaneous swimming test of larvae treated with various concentrations of GPR139 agonists. (A, B, and C) Kruskal–Wallis comparison between larvae treated with JNJ-63533054 (abbreviated as JNJ) in various concentrations and the control (0.1% DMSO) on (A) distance travel (millimeter, mm), (B) turn angle (degree), and (C) velocity (millimeter over second, mm/s). (D, E, and F) Kruskal–Wallis comparison between larvae treated with TAK-041 (abbreviated as TAK) in various concentrations and the control on (D) distance travel, (B) turn angle, and (C) velocity. ns indicates statistically non-significant.

Hence, JNJ and TAK at 50 μM did not influence the locomotion of larval zebrafish.

3.2 | Validation of Startle Habituation Paradigm

Startle stimuli were created by a series of vibrational forces caused by the tapping of an automated solenoid mounted close to the 24-well plate (Figure 2A). This setup was improvised from a previous single arena setup to increase the throughput [59]. A series of analyses were conducted to validate the solenoid setup and short-term startle habituation. To ensure the solenoid provided consistent startle strength to larvae located at different well positions ($n = 6$ per row of well), we compared the probability of response in a single habituation session between rows and found no significant difference in the Kruskal-Wallis test (Figure 2B: $H = 0.2746$, $p = 0.965$). Next, to rule out sensory and motor fatigue, we varied the interstimulus intervals (ISI: from 30 s to 1 s) of startle stimuli (Figure 2C). The probability of startle response remained high during the 30 s of ISI and dropped to and below 0.5 probability (0.4167) from the 11th trial onwards during the 1 s of ISI session. Such transition in behavioral response ruled out those potential confounds. Together, the new multiple-arena startle habituation setup showed validity in assessing the startle habituation of larval zebrafish with increased throughput.

We also quantified the short-term habituation trajectory using the exponential decay curve fit analysis (Figure 2H). The probability of response of the control group successively reduced across blocks of habituation (Figure 2D). Moreover, the amplitude, plateau, and tau of the exponential decay curve for the control group gradually decreased across blocks, showing adherence to characteristics of startle habituation as reported previously in zebrafish and other animal models [57, 61]. Some of the characteristics were evident in our paradigm. For

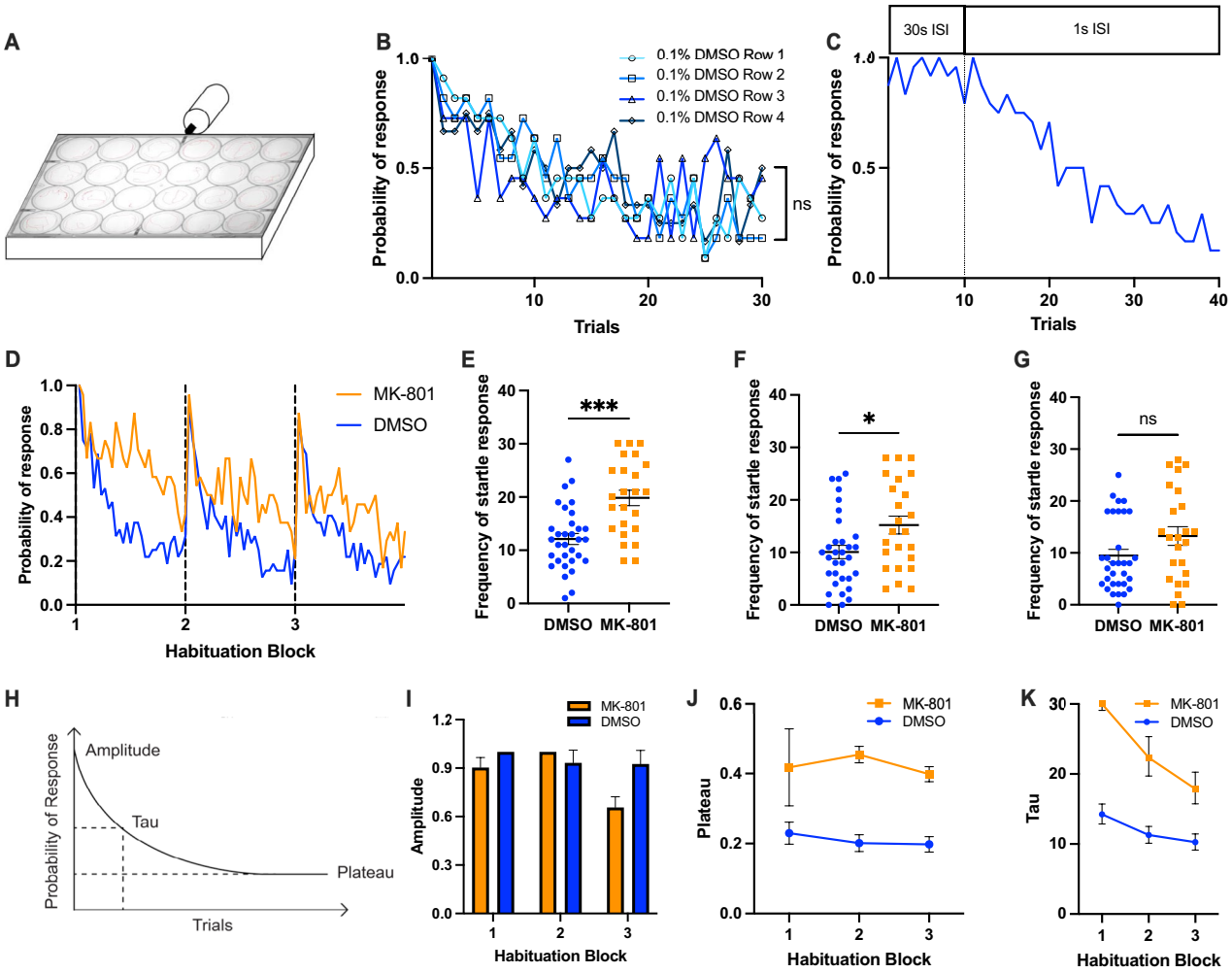

FIGURE 2 | Startle habituation paradigm setup and validation using MK-801-induced habituation impairment model. (A) The setup of startle habituation paradigm. The row of well closest to the solenoid was Row 1 and the furthest away was Row 4. (B) Probability of response of the larvae treated with 0.1% DMSO (same as the control) in different row position. (C) Probability of response of startle trials that transitioned from 30s interstimulus interval (ISI) to 1 s ISI. Gray dotted line separated the transition. (D) Probability of response of larvae treated with MK-801 (orange, abbreviated as MK) and in the control (blue). (E, F, and G) Mann–Whitney *U* test of startle frequency between the MK group and the control group in first, second, and third block of startle habituation, respectively. (H) Reference model of one-order exponential decay curve fit and the visualization of the extraction of amplitude, tau, and plateau parameters. (I, J, K) Using the first-order exponential decay curve analysis, the probability of startle response for each block and each group (the control and the MK group) was fitted to the mathematical model with different constraints to independently generate amplitude, plateau and tau values (see Method). Amplitude, plateau and tau of the exponential curve for the control and MK groups based on the respective probability of response. Horizontal bars represent mean and error bars represent SEM, except for K, in which the error bars represent 95% confidence interval. *** indicates $p < 0.001$, * indicates $p < 0.05$, and ns indicates non-significant difference.

instance, the control group showed a successive decrement in the probability of response across trials in each block; the amplitudes for three blocks had the highest probability of response within respective blocks, indicating spontaneous recovery (Figure 2I); plateau values that reduced across blocks showed the effect of habituation proceeded beyond the asymptotic level (Figure 2J); the tau values, which measured the time required for habituation in the session, were reduced across blocks, indicating potentiation of habituation (Figure 2K).

Prior to interpreting the effect of MK-801 on startle habituation, it was crucial to clarify the effect of MK-801 on locomotion. We tested the locomotion effect of MK-801 at 20 μM and 100 μM in larval zebrafish and found that 100 μM resulted in hypolocomotion (see Figure S1). To ensure the administration of MK-801 at 100 μM for 30 min was sufficient to disrupt startle habituation, we further compared various parameters with the control group. The larvae treated with MK-801 showed a significant elevation in the probability of response in the first two blocks (first block: $U = 157.5$, $p < 0.001$, Figure 2E; second block: $U = 244$, $p = 0.02$, Figure 2F; third block: $U = 286.5$, $p = 0.107$, Figure 2G). Persistent disruption to the characteristics of startle habituation in the MK group was found when comparing amplitude, plateau, and tau values with the control (Figure 2I–K). That was, the amplitude and plateau values of the exponential curve fluctuated (increased in value

from the first block, then decreased in value from the second block) across blocks, and the tau value remained higher than the control in all three blocks. These parameters showed failure in habituation learning. The disruptive effect of MK-801 was examined in the zebrafish and rodent models usually by reporting the frequency, percentage, or degree of habituation by comparing pre-test and post-test [48, 69–71]. We provided a detailed data visualization on how MK-801 disrupted startle habituation, which was most robustly in the first block (as seen in the frequency of startle response, Figure 2D,E), and plateau and tau remained higher than the control until the end of blocks, indicating persistent disruption of the characteristics of startle habituation.

3.3 | Effect of GPR139 Agonists on Startle Habituation

3.3.1 | JNJ-63533054 (JNJ)

Larvae treated with JNJ at different concentrations showed a varied probability of startle response (Figure 3A). In the first habituation block, the startle frequency of larvae treated with 1.6 μM and 20 μM of JNJ was not different from the control (Kruskal–Wallis test $H = 29.22$, $p < 0.001$, Dunn's multiple comparison tests showed at 1.6 μM $p = 0.152$, 20 μM $p = 0.476$, Figure 3B), whereas the startle frequency of larvae treated with 50 μM of JNJ was significantly higher than the control

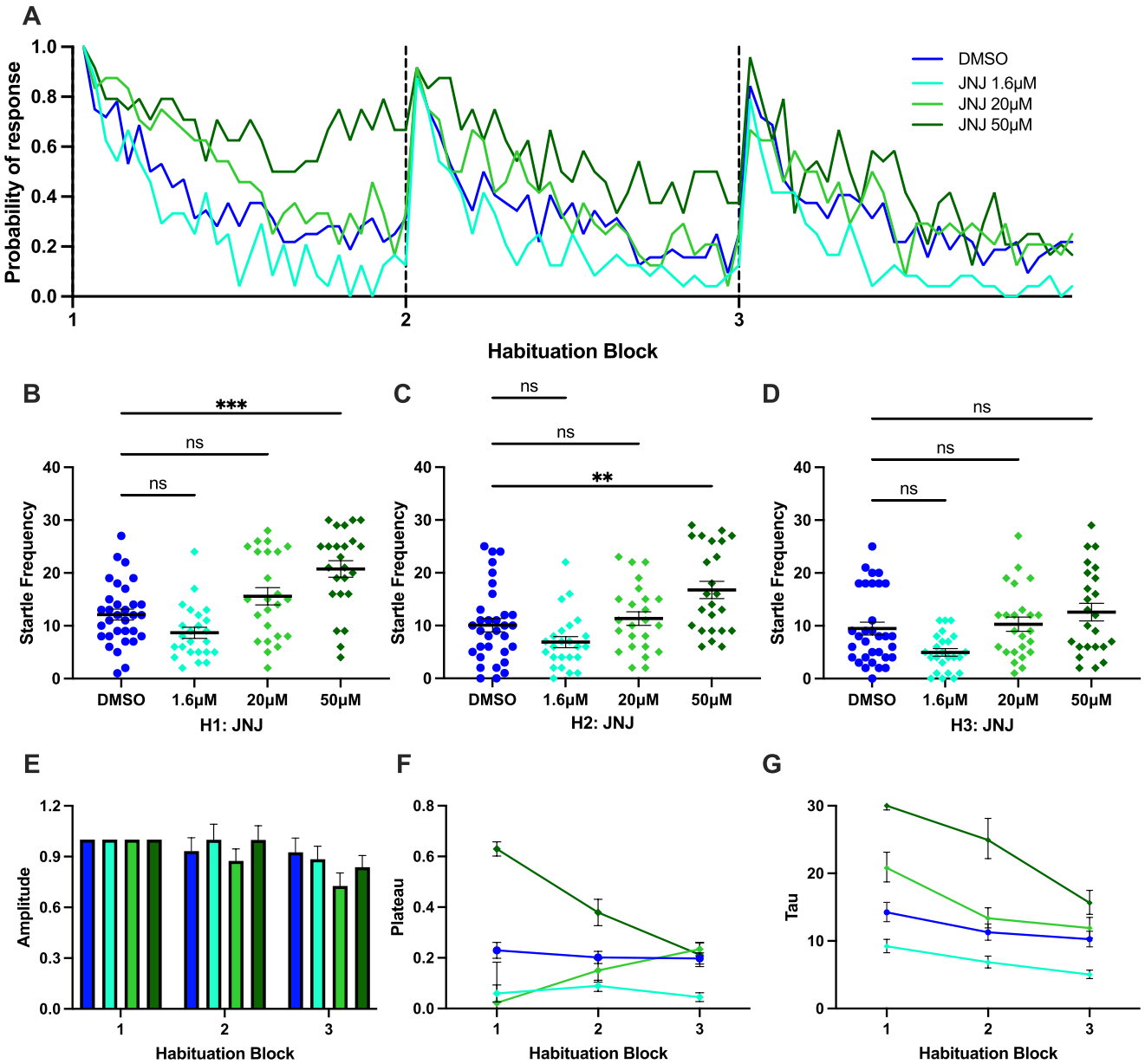

FIGURE 3 | Effect of JNJ-63533054 (abbreviated as JNJ) on startle habituation in larval zebrafish. (A) Probability of response of larvae treated with various concentrations of JNJ and the control in three habituation blocks. (B, C, D) Kruskal–Wallis test followed by Dunn's multiple comparison test on startle frequency of larvae treated with various concentrations of JNJ and the control in first, second, and third habituation blocks, respectively. (E, F, G) Amplitude, plateau and tau of the exponential curve for various concentrations of the JNJ group and the control group. Horizontal bars represent mean and error bars represent SEM, except for G, in which the error bar represents 95% confidence interval. *** indicates $p < 0.001$, ** indicates $p < 0.005$, and ns indicates non-significant difference.

($p < 0.001$). Similarly, in the second habituation block, larvae treated with 50 μM of JNJ continued to show higher startle frequency as compared to the control ($H = 21.43$, $p < 0.001$, Dunn's multiple comparison tests showed at 50 μM $p = 0.007$), whereas the larvae treated with the other two doses were not significantly different from the control (1.6 μM $p = 0.205$ and 20 μM $p > 0.999$, Figure 3C). Yet, in the third habituation block, larvae treated with all three doses did not show a significant difference in startle frequency as compared to the control ($H = 14.60$, $p = 0.002$, Dunn's multiple comparison tests showed for 1.6 μM, 20 μM, and 50 μM were $p = 0.057$, $p > 0.999$ and $p = 0.396$, Figure 3D).

We then conducted a first-order exponential decay curve fit analysis to quantify the parameters of the probability of response. Progressing from the first to third blocks, the amplitudes of the exponential curve in JNJ groups reduced across blocks, similar to the control group (Figure 3E). However, the plateau values of the exponential curve for JNJ groups were not similar to the control. The plateau values of 1.6 μM in three blocks were lower than 0.1 but slightly fluctuated with an increment in the second block. The plateau of 20 μM increased across blocks. The 50 μM of the JNJ group had a high plateau value of 0.63 in the first block and decreased across blocks (Figure 3F).

Next, the tau values of the exponential curve of all JNJ groups decreased from the first to the third blocks, with variation in each single block (Figure 3G). The tau value for the 50 μM JNJ group in the first block exceeded the constraint value of 30 and remained the highest among the JNJ groups in the second and third blocks. The tau values for the 20 μM JNJ group were lower than the 50 μM JNJ group in all blocks, whereas the tau values of the 1.6 μM JNJ group in all blocks were the lowest. The tau values for the 1.6 μM JNJ group in all blocks were the only values that were lower than the control.

3.3.2 | TAK-041 (TAK)

We also tested the effect of TAK on the startle habituation of larval zebrafish (Figure 4A). Within the first block of trials, there is no significant difference in the startle frequency of larvae treated with any doses of TAK as compared to the control ($H = 3.769$, $p = 0.288$; Figure 4B). Similarly, there was no effect of TAK on the startle frequency of larvae in the second habituation block ($H = 12.21$, $p = 0.007$; Figure 4C). On the other hand, in the third habituation block, the startle frequency of the larvae treated with 2.2 μM of TAK was significantly lower compared to the control ($H = 10.84$, $p = 0.013$, Dunn's multiple comparison tests showed at 2.2 μM $p = 0.014$; Figure 4D), whereas there was no difference in startle frequency of larvae treated with the other two doses and the control (20 μM: $p > 0.999$ and 50 μM: $p > 0.999$).

A further analysis of the probability of the response using the exponential decay curve fit analysis revealed that the amplitudes of the exponential curve for 2.2 μM and 50 μM TAK groups consistently decreased across the blocks of trials, with a larger magnitude of decrement being noticed in the 2.2 μM TAK group (Figure 4E). The amplitude for the 20 μM TAK group fluctuated across blocks with a small increment in the third block. The plateau of the exponential decay curve for the 2.2 μM, 20 μM TAK, and 50 μM groups decreased across the blocks of trials (Figure 4F). Among all plateau values, the 2.2 μM in the first block was higher than the control. The tau for three doses of TAK groups decreased across blocks, but the tau values of all groups were higher than the control in the first block. In the third block, the tau values for 2.2 μM and 20 μM TAK groups were lower than the control, whereas the 50 μM TAK group was higher than the control (Figure 4G).

Overall, similar to JNJ, treatment with TAK at the lowest concentration (2.2 μM) enhanced habituation. Although the lowest concentration of TAK resulted in a higher plateau and tau than the control in the first block, these parameters dropped lower than the control and were consistently observed in the second and third blocks. Treatment with 20 μM and 50 μM TAK affected the normal startle habituation as seen in fluctuated amplitude across blocks for the 20 μM TAK group and fluctuated plateau across blocks for the 50 μM TAK group. Comparing JNJ and TAK at their lowest concentrations, the 1.6 μM JNJ group had lower startle frequency than the 2.2 μM TAK group in the first block, but the difference ceased in the subsequent blocks $H = 53.32$, $p < 0.001$; Dunn's multiple comparison showed first block: $p < 0.001$, second and third blocks: $p > 0.999$; see Figure S1A.

3.4 | Effect of GPR139 Agonists on Impaired Startle Habituation Induced by MK-801

3.4.1 | Co-Treatment of JNJ-63533054 and MK-801 (MKJNJ)

We next investigated whether GPR139 agonists could reverse [29, 34] the disrupted startle habituation induced by MK-801 (referred to as MK; see Figure 2). We had previously confirmed that larvae exposed to MK could not habituate to startle stimuli normally. Whether GPR139 agonists could result in a normal habituation performance on MK-induced larvae is considered a reversal in disrupted startle habituation. The overview of the probability of response of the JNJ-treated group and MK group was illustrated in Figure 5A. The startle frequency of larvae co-treated with MK and JNJ (abbreviated as MKJNJ) was significantly lower in the first block as compared to the MK group ($H = 27.14$, $p < 0.001$, Dunn's multiple comparison tests showed for 1.6 μM, 20 μM and 50 μM were $p < 0.001$, Figure 5B). Similarly, in the second and third blocks, the MK group exhibited a high level of startle frequency throughout the habituation trials, which was diminished in larvae co-treated with JNJ. However, this effect was not seen in the group co-treated with MK, and the highest dose (50 μM) of JNJ (second habituation block, $H = 25.96$, $p < 0.001$, Dunn's multiple comparison tests showed for 1.6 μM, $p < 0.001$, 20 μM, $p < 0.001$ and 50 μM, $p = 0.119$, Figure 5C; third habituation block, $H = 22.97$, $p < 0.001$, Dunn's multiple comparison tests showed at 1.6 μM, $p = 0.001$, 20 μM, $p < 0.001$ and 50 μM, $p = 0.209$, Figure 5D).

The amplitude of the exponential curve for 50 μM and 20 μM MKJNJ groups fluctuated across blocks, whereas the amplitude for 1.6 μM MKJNJ group decreased across blocks (Figure 5E). The plateau for 1.6 μM and 20 μM MKJNJ groups decreased

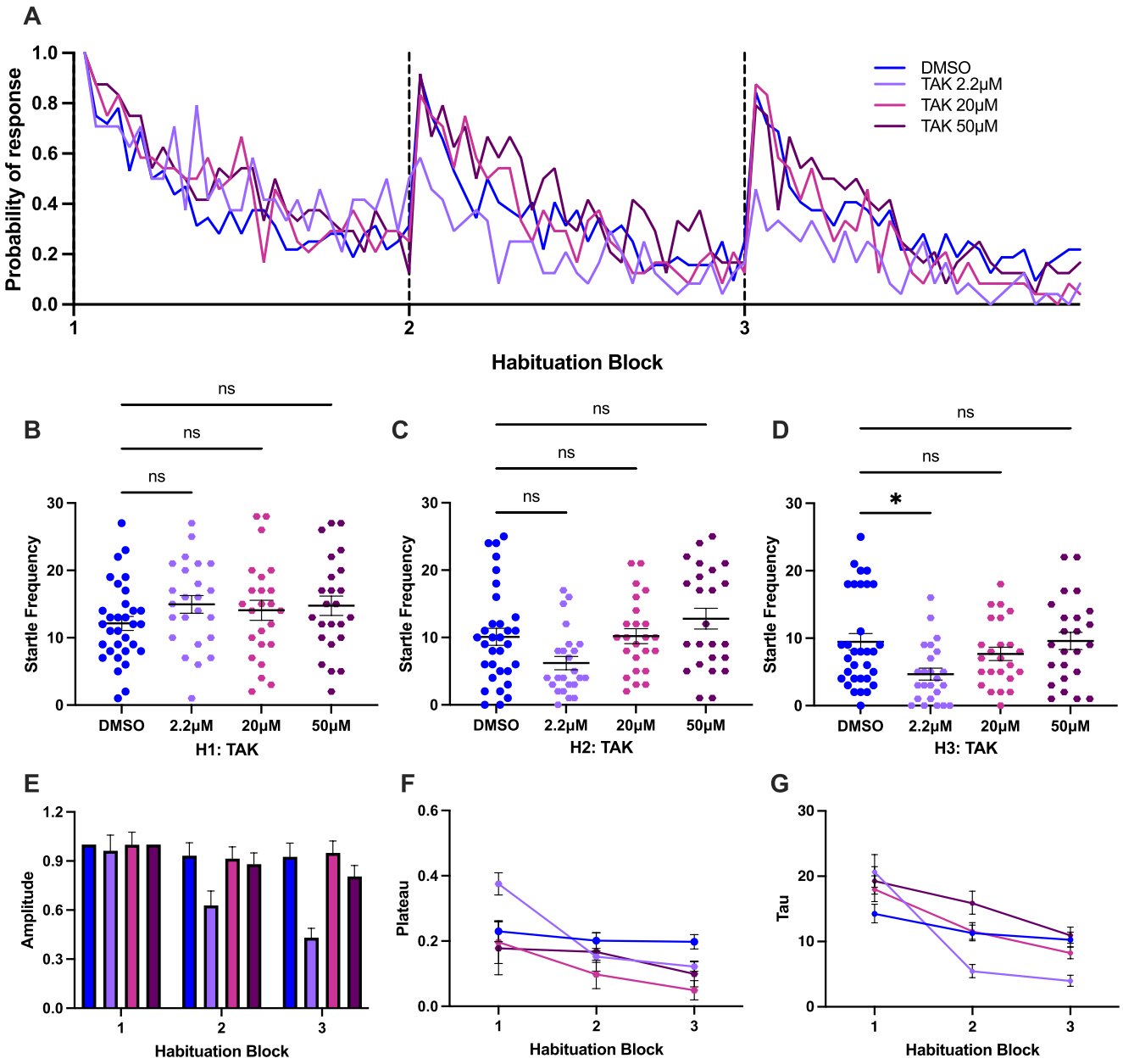

FIGURE 4 | Effect of TAK-041 (abbreviated as TAK) on startle habituation in larval zebrafish. (A) Probability of response of larvae treated with various concentrations of TAK and the control in three habituation blocks. (B, C, D) Kruskal–Wallis test followed by Dunn's multiple comparison test on startle frequency of larvae treated with various concentrations of TAK and the control in first, second, and third habituation blocks, respectively. (E, F, G) Amplitude, plateau and tau of the exponential curve for various concentrations of the TAK groups and the control group. Horizontal bars represent mean, and error bars represent SEM, except for G, in which the error bars represent 95% confidence interval. * indicates $p < 0.05$, and ns indicates non-significant difference.

across blocks, whereas the plateau for 50 μM MKJNJ group fluctuated across blocks (Figure 5F). The tau for 1.6 μM MKJNJ group decreased across blocks, whereas the tau for 20 μM and 50 μM MKJNJ groups fluctuated across blocks (Figure 5G).

3.4.2 | Co-Treatment of TAK-041 and MK-801 (MKTAK)

The probabilities of the response of the larvae co-treated with MK-801 and TAK-041 and the MK-801 group are shown in Figure 6A. The startle frequencies of larvae in three doses of MKTAK groups were significantly lower than the MK-801 group in all three habituation blocks (the first habituation block: $H = 34.68$, $p < 0.001$, Dunn's multiple comparison tests showed that 2.2 μM, 20 μM, and 50 μM were $p < 0.001$, Figure 6B; second habituation block: $H = 31.39$, $p < 0.001$, Dunn's multiple comparison tests showed that 2.2 μM, 20 μM, and 50 μM were $p < 0.001$, Figure 6C; third habituation block: $H = 22.89$, $p < 0.001$, Dunn's multiple comparison tests showed at 1.6 μM, $p < 0.001$, 20 μM, $p = 0.003$ and 50 μM, $p < 0.001$, Figure 6D).

The amplitude of the exponential curve for 2.2 μM and 20 μM MKTAK groups consistently decreased across the blocks, with the amplitude in the second and third blocks lower than those in

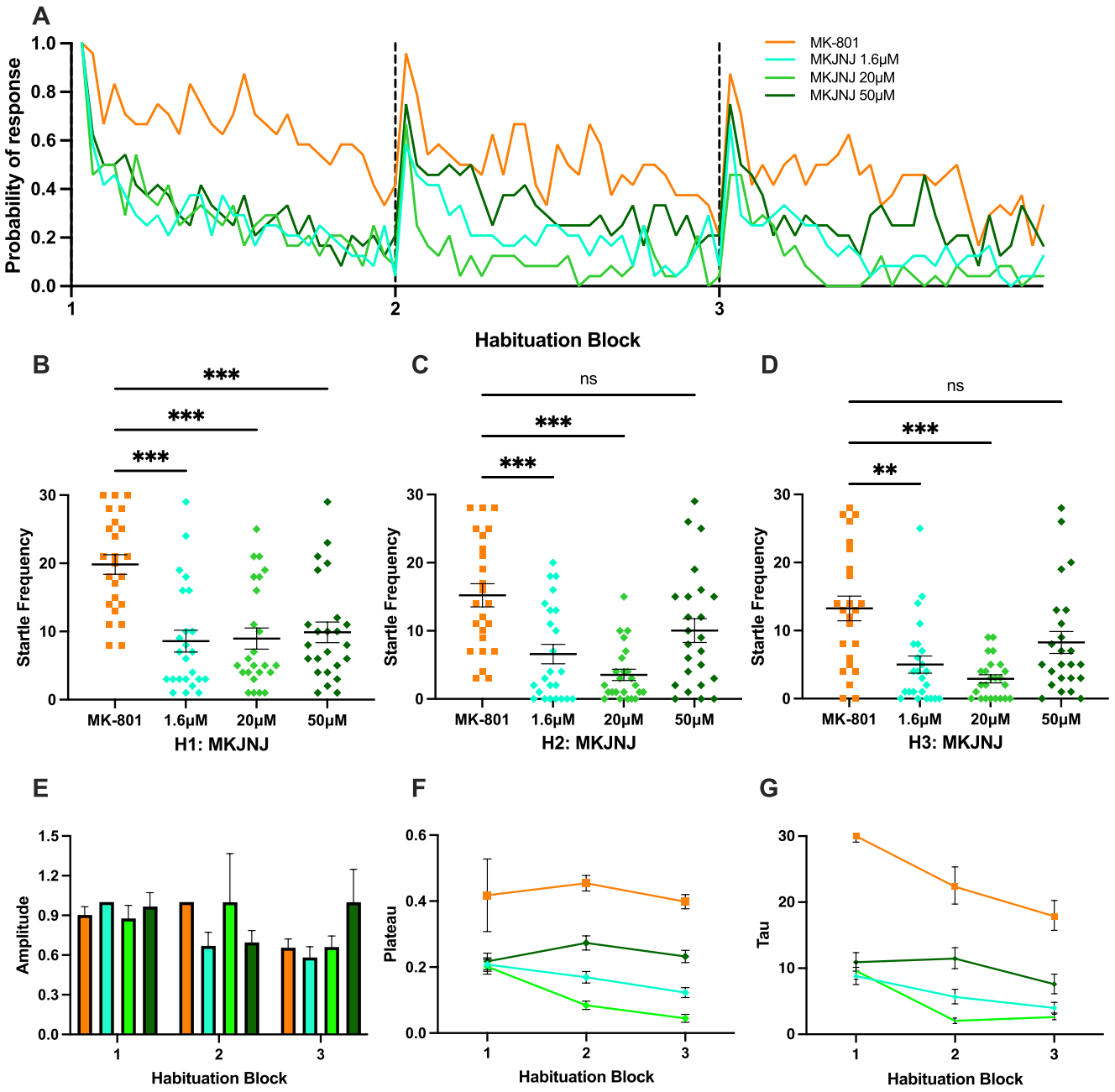

FIGURE 5 | Effect of JNJ-63533054 on MK-801-induced larval zebrafish in startle habituation paradigm. (A) Probability of response of MK-801-induced larvae treated with various concentrations of JNJ-63533054 (abbreviated as MKJNJ) and MK-801-treated (abbreviated as MK) groups in three habituation blocks. (B, C, D) Kruskal–Wallis test followed by Dunn's multiple comparison test on startle frequency of MKJNJ group in first, second, and third habituation blocks, respectively. (E, F, G) Amplitude, plateau and tau of the exponential curve for various concentrations of the MKJNJ group and the MK group. Horizontal bars represent mean, and error bars represent SEM, except for G, in which the error bars represent 95% confidence interval. *** indicates $p < 0.001$, ** indicates $p < 0.005$, and ns indicates non-significant difference.

the control group, whereas the amplitude for the 50 μM MKTAK group remained unchanged across blocks (Figure 6E). The plateau for the 2.2 μM and 20 μM MKTAK groups decreased across the blocks, whereas the plateau for the 50 μM MKTAK group fluctuated across blocks (Figure 6F). The tau values for all tested concentrations showed a decreasing trend and were lower than the MK group across blocks, with the 2.2 μM and 20 μM slightly fluctuating and increasing in the last block (Figure 6G). Overall, while TAK-041 reversed the disruption caused by MK-801, only the lowest concentration (2.2 μM) retained all the proper characteristics of startle habituation, which was observed from decreasing amplitude, plateau, and tau values across blocks from the exponential decay curve fit analysis.

Comparing MKJNJ and MKTAK groups at their lowest concentrations showed that the MKTAK group had a lower startle frequency than the MKJNJ group in the third block only ($H = 42.87$, $p < 0.001$, Dunn's multiple comparisons showed $p = 0.038$, whereas the first and second block showed $p = 0.279$, $p = 0.082$ see Figure S1B).

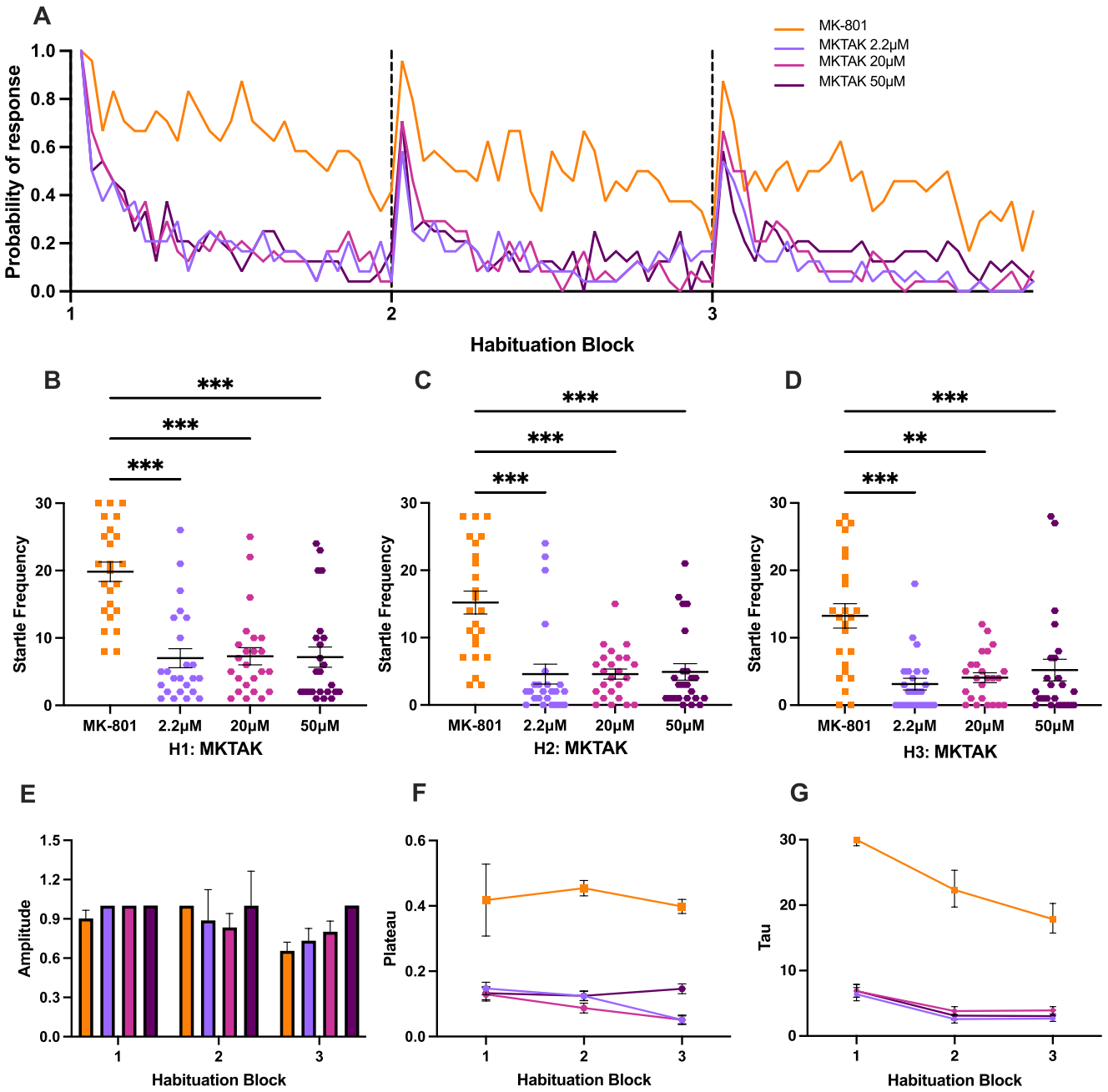

FIGURE 6 | Effect of TAK-041 on MK-801-induced larval zebrafish in startle habituation paradigm. (A) Probability of response of MK-801-induced larvae treated with various concentrations of TAK-041 (abbreviated as MKTAK) and the MK group in three habituation blocks. (B, C, D) Kruskal-Wallis test followed by Dunn's multiple comparison test on startle frequency of MK-801-induced larvae treated with various concentrations of TAK and the MK group in first, second, and third habituation blocks, respectively. (E, F, G) Amplitude, plateau and tau of the exponential curve for various concentrations of the MKTAK group and the MK group. Horizontal bars represent mean, and error bars represent SEM, except for G, in which the error bars represent 95% confidence interval. *** indicates $p < 0.001$, and ** indicates $p < 0.005$.

3.5 | Effect of GPR139 Agonists and MK-801 on Spontaneous Neural Activities in the Habenula

In zebrafish, gpr139 is only expressed in the ventral habenula and has been shown to mediate cognitive functions such as fear learning [34]. However, much remains unknown about the role of GPR139 signaling in the habenula. Since only a limited number of studies have examined the effect of GPR139 agonists on habenula neural activity, we conducted calcium imaging on the baseline spontaneous activity of the 6 dpf *Tg(HuC:Gal4VP16;UAS:GCaMP6s)* zebrafish. Based on the conclusion of the behavioral data, we used the lowest concentration, which was 1.6 μM for JNJ-63533054 and 2.2 μM for TAK-041. We recorded a single plane of the whole habenula at a depth of $M = 24.065\,\mu m$ (SD = 2.98 μm) from the dorsal surface of the habenula (Figure 7A). The habenula activity before and 20 min after the administration of GPR139 agonists was recorded for 3 min and 9 min, respectively, to follow the same drug-exposure time schedule used in the behavioral experiment.

After 20 min of exposure to compounds, the habenula cells change in firing activity compared to before exposure (Figure 7B,E,H). Compared to the mean fluorescence intensity ($\Delta F/F_0$) before exposure, we identified three types of cell profiles that have increased activity (M + 2SD higher than the mean fluorescence intensity before exposure), decreased activity (M + 2SD lower), and no change in activity. The JNJ group had a different cell profile than the TAK group. Similar to the control (the majority 48.98% increase in activity, Figure 7I), the majority of neural cells in the TAK group increased in activity (49.88%, Figure 7F). The JNJ group had a majority of neural cells with decreased activity (48.44%, Figure 7C). Despite the change in cell profile, the frequency and average

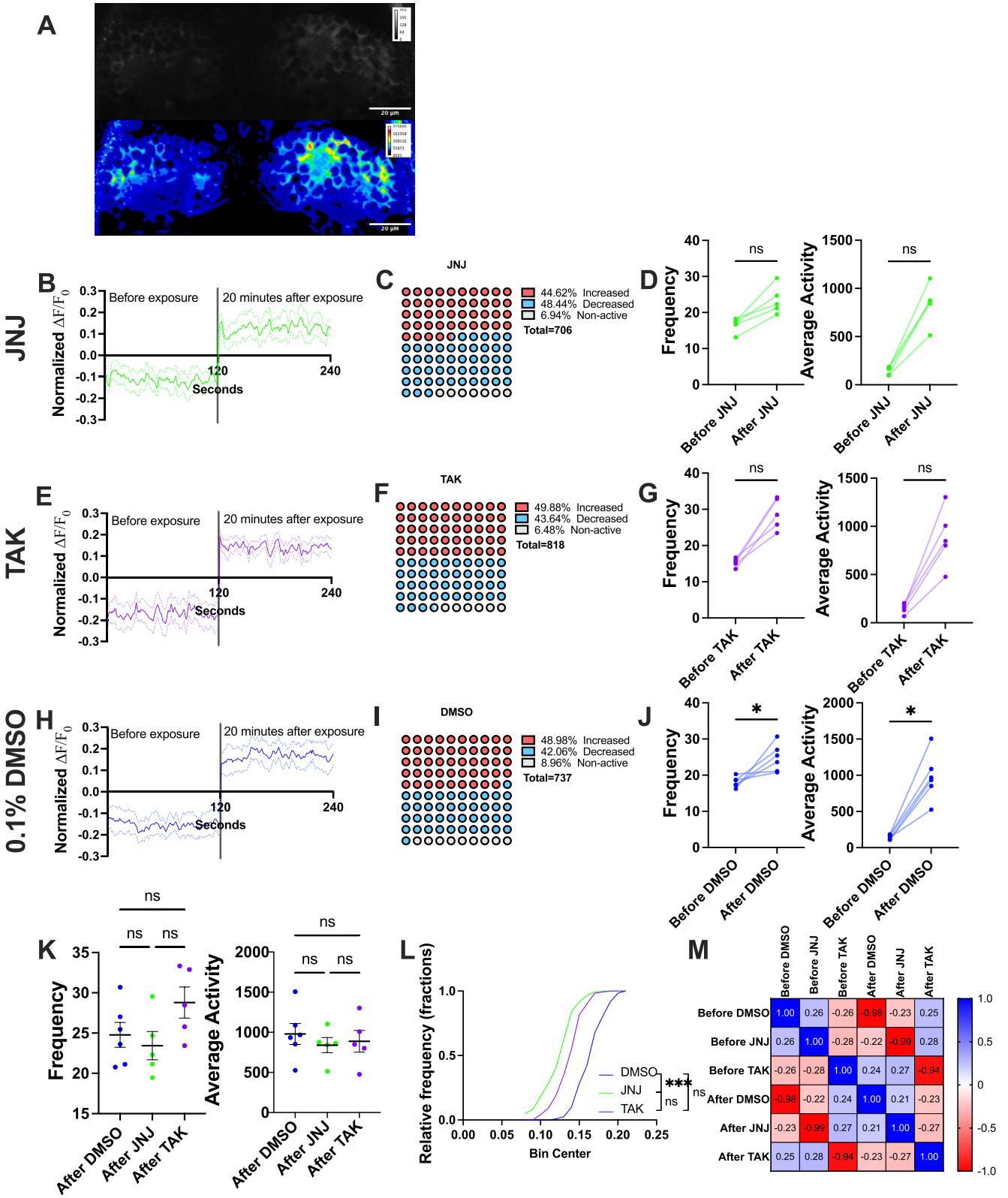

FIGURE 7 | Legend on next page.

FIGURE 7 | Spontaneous activity of habenula of larvae treated with GPR139 agonists. (A) Sample image of habenula in gray (top) extracted from maximum intensity projection and in color (bottom) extracted from sum slice projection. Scale bar indicated as 20 μM. (B, E, H) Normalized mean fluorescence intensity ($\Delta F/F_0$) of the JNJ (B), TAK (E), and the control (H) groups 120 s before compound exposure (pre-) and 20-min after exposure (post-). The vertical line indicated the separation of both conditions. Solid line was the mean value, and dashed lines were the SEM (C, F, and I) Percentage of the neurons with increased, decreased, and no change in fluorescence intensity in post-exposure condition compared to the mean value of fluorescence intensity in pre-exposure condition. (D, G, J) Mean frequency (left) and mean average activity (right) of pre- and post-eposure conditions and pairwise comparison with Wilcoxon test. (K) Mean frequency and mean average activity and Kruskal–Wallis test, followed by Dunn's multiple comparison test between JNJ, TAK, and the control groups. Mean in thick horizontal line and SEM in error bars were illustrated. (L) Cumulative distribution of fluorescence intensity in fractions in post-exposure condition and Kruskal–Wallis test with Dunn's multiple comparison test. (M) Correlation matrix of fluorescence intensity for JNJ, TAK, and the control in pre- and post-exposure conditions. * indicated $p < 0.05$, *** indicated $p < 0.001$, and ns indicated non-significant difference.

activity in the after condition were not significantly different from the before condition in the Wilcoxon paired test in the JNJ group (Frequency: $T = 15$, $n = 5$, $p = 0.062$; average activity: $T = 15$, $n = 5$, $p = 0.062$, Figure 7D) and TAK group (Frequency: $T = 15$, $n = 5$, $p = 0.062$; average activity: $T = 15$, $n = 5$, $p = 0.062$, Figure 7G), except for the control where the after condition was higher than the before condition in both frequency ($T = 21$, $n = 6$, $p = 0.031$) and average activity ($T = 21$, $n = 6$, $p = 0.031$, Figure 7J).

Between-group comparison also did not reveal significant changes in neural activity in the JNJ and TAK groups compared with the control (Frequency: $H(16) = 3.753$, $p = 0.159$; average activity: $H(16) = 0.953$, $p = 0.650$, Figure 7K). We then considered whether the neurophysiological effect of JNJ-63533054 and TAK-041 was progressive over time. We compared the cumulative difference and found that the JNJ group had a significantly higher neural activity compared with the control ($H(2) = 24$, $p < 0.001$; Dunn's multiple comparison tests showed JNJ: $p < 0.001$; TAK: $p = 0.07$, Figure 7L). The correlation matrix of neural activity revealed that the control had a positive relationship with the JNJ group and a negative relationship with the TAK group (Figure 7M).

3.5.1 | The Effect of JNJ-63533054 and TAK-041 With the Presence of MK-801

We next examined the MK-801-altered spontaneous activity of the habenula under the exposure of JNJ-63533054 and TAK-041. We first recorded a 3-min spontaneous activity of the habenula exposed to MK-801 (see neural activity before and after MK-801 exposure, Figure 8A), followed by a 9-min recording of MK-801, then another 9-min recording of the co-treatment of MK-801 and GPR139 agonists exposure (Figure 8B,D). MK-801 decreased most neural activity (58.25% and 49.69%) compared to before exposure (Figure 8C left, E left). The cells profile remained the same even with the co-treatment of MK-801 and JNJ-63533054 (59.34% decreased activity) or TAK-041 (73.54%) compared to MK-801 exposure alone (Figure 8C right, E right). However, pairwise comparison failed to show significance in frequency and average activity when comparing before and after MK-801 exposure in two group replicates (MK for MKJNJ: frequency, $T = 2$, $n = 7$, $p = 0.938$; average activity, $T = 0$, $n = 7$, $p > 0.999$, Figure 8F (i); MK for MKTAK: frequency, $T = 13$, $n = 5$, $p = 0.125$; average activity, $T = -11$, $n = 5$, $p = 0.188$, Figure 8F (ii)).

A small significant increment in mean frequency and mean average activity was observed only in the MKJNJ group in pairwise comparison with the MK group (frequency: $T = 26$, $n = 7$, $p = 0.031$; average activity: $T = 28$, $n = 7$, $p = 0.016$, Figure 8F (ii)). The MKTAK group did not alter the neural activity induced by MK-801 (frequency: $T = 7$, $n = 5$, $p = 0.438$; average activity: $T = 15$, $n = 5$, $p = 0.062$, Figure 8G (ii)). The cumulative difference showed the MKJNJ group reached the ceiling plateau slower than its MK group ($T = -136$, $n = 17$, $p < 0.001$), whereas the MKTAK was slower than its MK group ($T = 300$, $n = 25$, $p < 0.001$, Figure 8H). However, the correlation matrix showed a congruent pattern for the MKJNJ and MKTAK groups, as both groups were negatively correlated with the respective MK groups (Figure 8I).

3.6 | Effect of GPR139 Agonists on Habenula Activities at Habituated State

We next examined the effect of GPR139 agonists on the habenula activity at a habituated state. After the startle habituation paradigm, we proceeded with pERK immunohistochemistry (Figure 9A). We recorded the z-stack of the habenula and analyzed three planes with 7 μm apart. Exposure to JNJ and TAK agonists reduced the pERK/tERK-immunofluorescence intensity at the lower plane of the habenula compared to plane 1 (closest to the surface) (JNJ: $\chi^2(2) = 18.84$, $p < 0.001$; plane 1 vs. plane 2, $p = 0.226$; plane 2 vs. plane 3, $p < 0.001$, plane 1 vs. plane 3, $p = 0.033$, Figure 9C; TAK: $\chi^2(2) = 34.32$, $p < 0.001$; plane 2 vs. plane 3, $p = 0.612$; plane 3 vs. plane 4, $p < 0.001$, Figure 9D), whereas the control did not differ in intensity among planes ($\chi^2(2) = 3.355$, $p = 0.187$, Figure 9B).

In the cumulative distribution, the JNJ and TAK groups reached the ceiling plateau slower than the control ($H(2) = 152.3$, $p < 0.001$; JNJ vs. DMSO: $p < 0.001$; TAK vs. DMSO: $p < 0.001$; JNJ vs. TAK: $p < 0.001$, Figure 9E). Combining three habenula planes, JNJ and TAK agonists showed higher intensity compared to the control ($\chi^2(2) = 19.42$, $p < 0.001$, Dunn's multiple comparison test for JNJ: $p < 0.001$ and TAK: $p < 0.001$, Figure 9F). We noticed that the ventral region of the left and right habenula had a higher intensity than the dorsal region in the slope of linear regression of the control group. The slope of the linear regression increased in the JNJ and TAK groups compared to the control (Figure 9G).

3.6.1 | Effect of JNJ-63533054 and TAK-041 on Startle Habituation With the Presence of MK-801

Next, we examined the effect of GPR139 agonists on MK-801-induced habenula in a habituated state in pERK

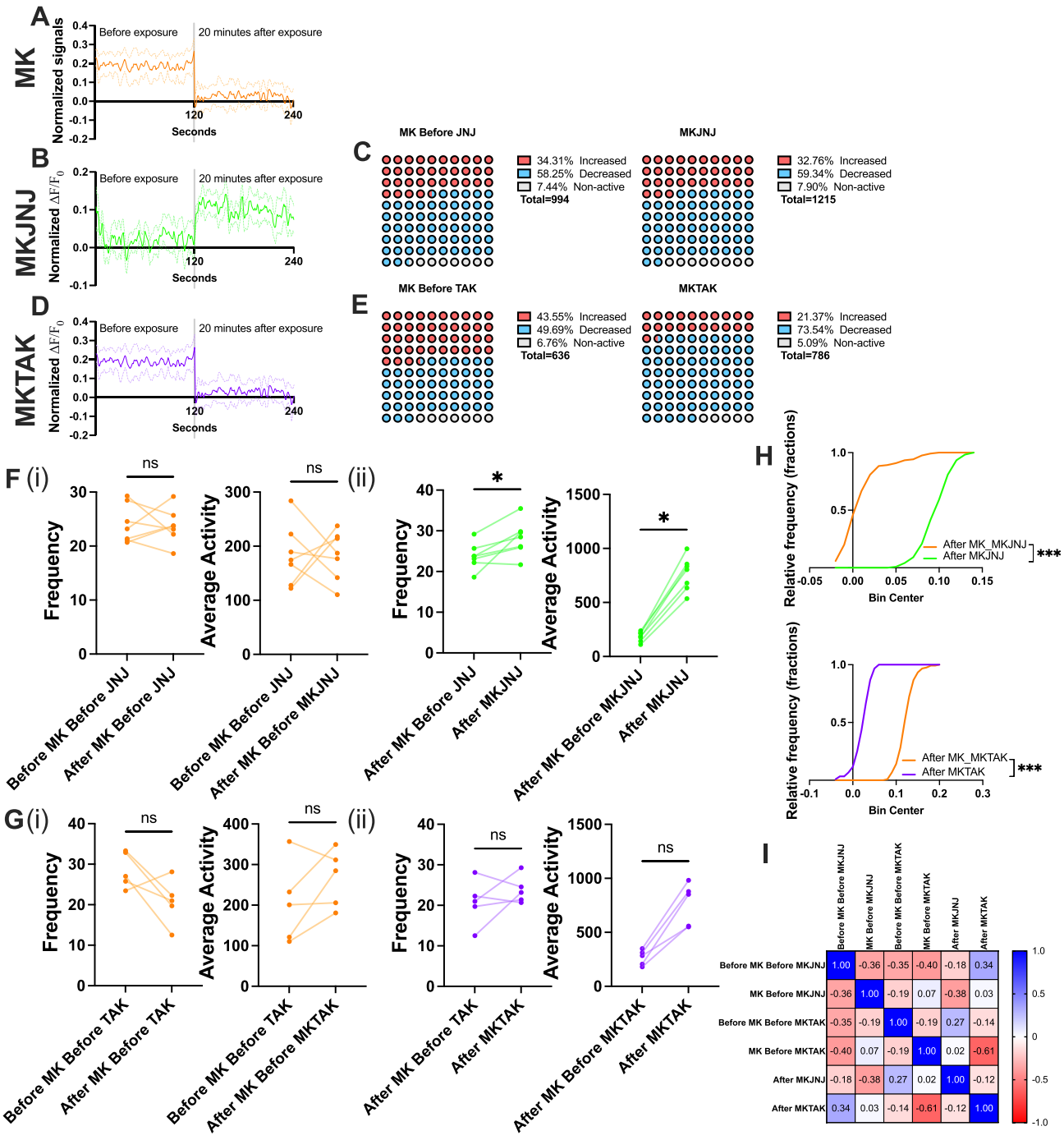

FIGURE 8 | Spontaneous activity of habenula of MK-801-induced larvae treated with GPR139 agonists. (A, B, D) Normalized mean fluorescence intensity ($\Delta F/F_0$) of GCaMP signals in the MK (A), MKJNJ (B), and MKTAK (D) groups 120 s before compound exposure and 20-min after exposure. The vertical line indicated the separation of both conditions. Solid line was the mean value, and dashed lines were the SEM (C and E) Percentage of the neurons with increased, decreased, and no change in fluorescence intensity in MK-801-induced condition (left) and 20 min after GPR139 agonists exposure, comparing to the mean value of fluorescence intensity in pre-exposure condition. (F and G) Pairwise comparison with Wilcoxon test on mean frequency and mean average activity of before and after MK-801 exposure (F, i, G i) and before and after JNJ-63533054 (F, ii) and TAK-041 (G, ii) exposure to MK-801-induced larvae. (H) Cumulative distribution of fluorescence intensity in fractions in post-exposure condition for MKJNJ (top) and MKTAK (bottom) and the Kruskal–Wallis test followed by Dunn's. (I) Correlation matrix of $\Delta F/F_0$ for MKJNJ, MKTAK, and the MK group in pre- and post-exposure conditions. * indicated $p < 0.05$, *** indicated $p < 0.001$, and ns indicated non-significant difference.

immunohistochemistry (Figure 10A). The MK group has no difference in the pERK/tERK ratio in different depths of planes ($\chi^2(2) = 4.065$, $p = 0.131$, Figure 10B). The difference in the pERK/tERK was noticed only between plane 1 and plane 2 of both the MKJNJ and MKTAK groups (MKJNJ: $\chi^2(2) = 7.032$, $p = 0.03$; plane 2 vs. plane 3, $p = 0.093$; plane 3 vs. plane 4, $p > 0.999$, plane 2 vs. plane 4, $p = 0.047$, Figure 10C; MKTAK: $\chi^2(2) = 7.548$, $p = 0.023$; plane 2 vs. plane 3, $p = 0.170$; plane 3 vs. plane 4, $p > 0.999$, plane 2 vs. plane 4, $p = 0.023$, Figure 10D). The cumulative distribution difference revealed

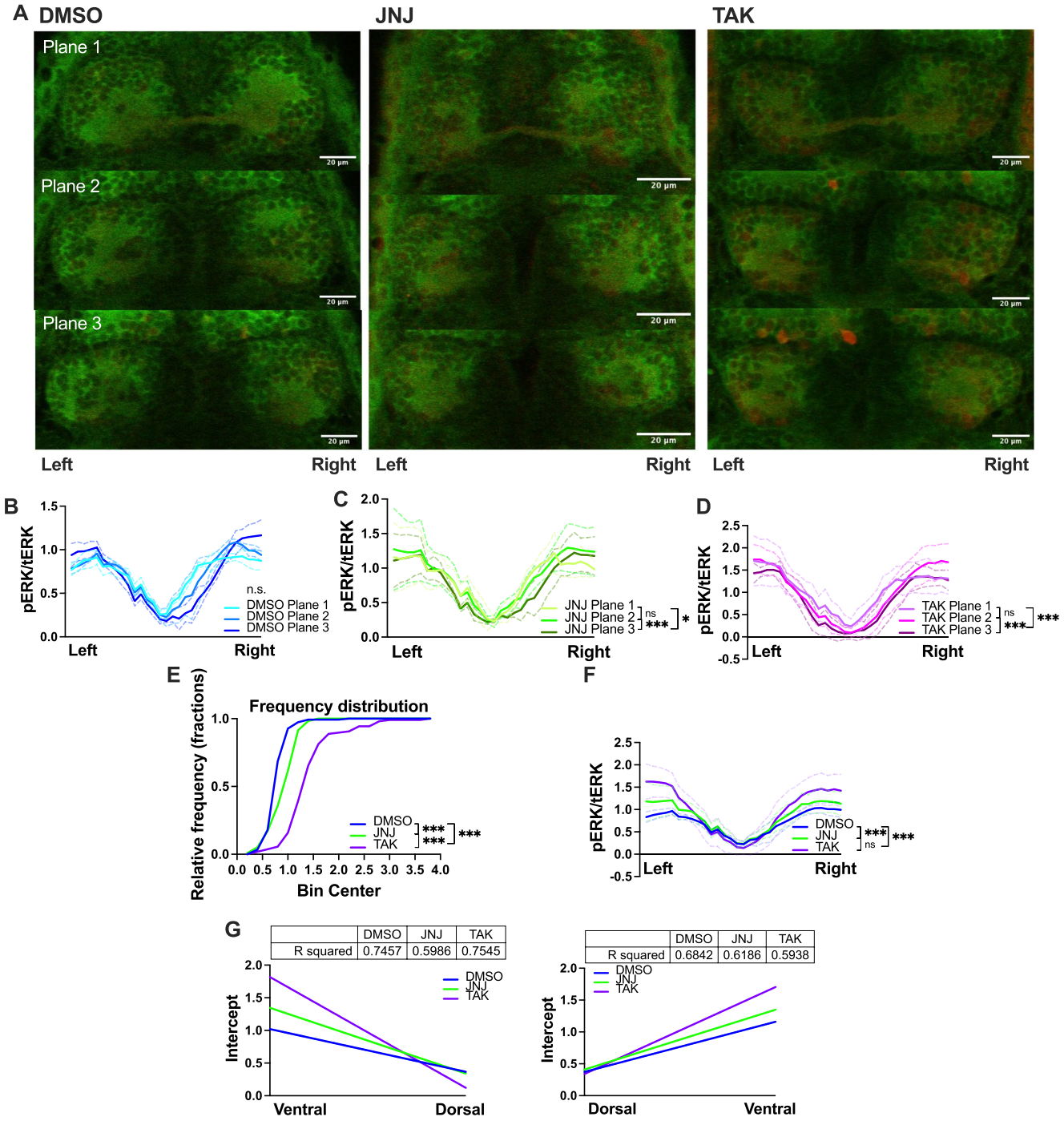

FIGURE 9 | pERK (green)/tERK (red)-signals of normal larval zebrafish habenula after the startle habituation paradigm. (A) Sample illustration of three z planes separated by 7 μM for the control (left), JNJ (middle) and TAK (right) groups. White scale bar: 20 μM (B, C, D) pERK/tERK values of three planes arranged the ventral side of the left habenula (labeled as left) to the ventral side of the right habenula (labeled as right). (E) Cumulative distribution in fractions of pERK/tERK values of the control, JNJ and TAK groups. (F) Comparison of combined planes pERK/tERK between groups. (G) Linear regression for left habenula (left) and right habenula (right). Kruskal–Wallis test followed by Dunn's multiple comparison test were conducted. *R* squared of the fitted line were tabled. * indicated $p < 0.05$, *** indicated $p < 0.001$, and ns indicated non-significant difference.

that the MKJNJ and MKTAK groups reached the ceiling plateau earlier than the MK groups ($H(2) = 129.2$, $p < 0.001$; MKJNJ vs. MK, $p < 0.001$; MKTAK vs. MK, $p < 0.001$; MKJNJ vs. MKTAK, $p = 0.227$, Figure 10E). Combining three planes, the MKJNJ and MKTAK groups showed a lower pERK/tERK ratio compared to the MK group ($\chi^2(2) = 51.16$, $p < 0.001$, Dunn's multiple comparison test for MKJNJ vs. MK: $p < 0.001$; MKTAK vs. MK: $p < 0.001$; MKJNJ vs. MKTAK, $p = 0.093$, Figure 10F). Fitting ventral to dorsal pERK/tERK ratio for both left and right habenula in linear regression showed that the MK group had the highest intercept value. In the left habenula, the slope of the fitted line was higher in the MKJNJ and MKTAK groups than in the MK group. In the right habenula, the slope was the highest in the MKJNJ

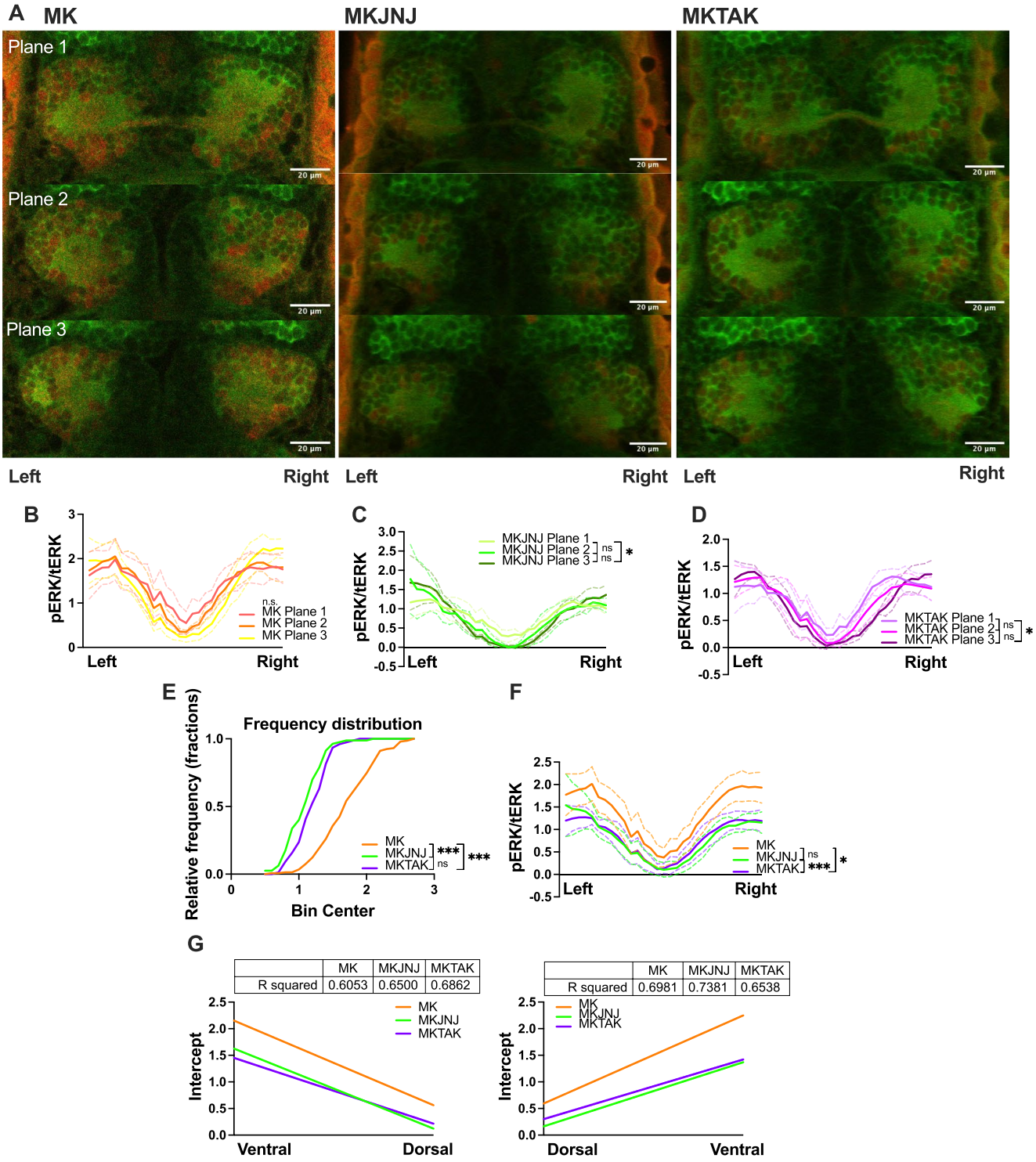

FIGURE 10 | pERK (green)/tERK (red)-signals of MK-801-induced larval zebrafish habenula after the startle habituation paradigm. (A) Sample illustration of three z planes separated by 7 μM for the MK (left), MKJNJ (middle) and MKTAK (right) groups. White scale bar: 20 μM (B, C, D) pERK/tERK values of three planes arranged the ventral side of the left habenula (labeled as left) to the ventral side of the right habenula (labeled as right). (E) Cumulative distribution in fractions of pERK/tERK values of the MK, MKJNJ and MKTAK groups. (F) Comparison of combined planes pERK/tERK between groups. (G) Linear regression for left habenula (left) and right habenula (right). *R* squared of the fitted line were tabled. Kruskal–Wallis test followed by Dunn's multiple comparison test were conducted. * indicated $p < 0.05$, *** indicated $p < 0.001$, and ns indicated non-significant difference.

group, followed by the MK group and then the MKTAK group. Exposure to JNJ-63533054 and TAK-041 in the presence of MK-801 increased the slope values (Figure 10E), suggesting a higher activation in the ventral region.

4 | Discussion

GPR139 has recently been implicated in understanding neurobehavior and neuropsychiatric disorders, especially the negative

and cognitive symptoms of schizophrenia [29, 30, 41]. Despite several GPR139 agonists, such as JNJ-63533054 and TAK-041, having shown their positive effects on improving cognitive and social dysfunctions in animal models [30], much remained unknown about how the activation of GPR139 signaling in the habenula could affect cognitive functions associated with schizophrenia. In the present study, we elucidate the role of GPR139 signaling in habenula activity and its effect on cognitive performance using the startle habituation deficit model in larval zebrafish.

The improved startle habituation setup from [59] demonstrated a consistent delivery of stimulus strength to larvae in all wells even though only one solenoid was attached to a side of the wall. The solenoid was tested to provide sufficient vibrational strength to startle larvae but not overly strong, as larvae would not habituate under an overly intensive condition [57]. Although acoustic stimuli are commonly used as startle stimuli in larval zebrafish [72, 73], most experimental setups utilized a speaker to vibrate the plate attached beneath the well, which was similar to the vibrational force of a tapping solenoid. In addition, vibrational startle stimuli similarly induce startle responses to acoustic stimuli [61]. Therefore, with the commercially available solenoid and the standard 24-well plate, this improved setup is capable of providing moderate throughput for larval zebrafish behavioral experiments.

Startle habituation is defined as a decrement in startle response over repetitive startle stimulation, with the behavioral trajectory adhering to the characteristics of startle habituation [57, 61]. The startle response in zebrafish triggered by acoustic or vibrational stimuli is typically observed with a sequential Short Latency C-start, SLC, followed by the Long Latency C-start LLC [47, 74]. The SLC response was probabilistic and ceased shortly, whereas the LLC, which was likely observed in low-intensity stimulation, maintained responsiveness as a backup escape response [75]. The SLC is mediated by a well-defined neural circuit in the brainstem and spinal cord; a major component of this circuit is a small number of hindbrain neurons, which are the large, bilaterally paired Mauthner cells [76]. Startle habituation of the SLC is regulated by the suppression of Mauthner neuron excitability in the locomotor circuit [77]. The suppression signal can be strengthened from NMDA receptor-dependent feedforward neurons to the lateral dendrite activity of Mauthner neurons [70]. The startle probability regulation by the NMDA receptor was observed in the spaced-training paradigm (short-term and long-term habituation) but not in the single-session paradigm [47, 78]. The SLC response mediated by the Mauthner network is crucial for understanding the startle habituation mechanism. This mechanism may be associated with habenular signaling; however, the potential link between the habenula and the Mauthner neurons requires further investigation. We understood that only a 30 Hz video recording could not distinguish the SLC from the LLC response, as both responses happened before 30 ms [75]. However, our computational analysis on the probability of startle response, which measured body-position change, provided the result of a rapid decline in startle response that can be reinitiated in subsequent blocks, ensuring the capability to collect the SLC response (with also LLC response) that presented the nature of startle habituation. Hence, our paradigm could effectively exhibit startle habituation in larval zebrafish.

In modeling larval zebrafish with startle habituation deficit, we found that exposure to MK-801 caused disruption to the short-term startle habituation in 6 dpf larvae as reported previously [47, 48, 59]. MK-801 was found to affect SLC response decrement in habituation but not the SLC behavioral mechanism [48], suggesting that MK-801-induced larvae could still habituate, but the normal mechanism was impaired. Our study showed that MK-801-induced larvae reached a decreased probability of response near the end of trial blocks, but the rate of habituation was largely impaired. It could be speculated that MK-801 could have disrupted the startle habituation mechanism in the upstream pathway instead of the Mauthner network that mediated behavioral response. MK-801 induced different habenula neural activity at both the idle state (before the startle habituation paradigm) and after the startle habituation paradigm. At the idle state, we found that MK-801 exposure resulted in hypoactive spontaneous activity. However, the pERK immunostaining showed hyperactivation in the overall habenula of the MK-801-treated larvae. Pairing both the behavioral and cellular activity observations, it is possible that the impairment of habituation induced by MK-801 is associated with disrupting the baseline activity of the habenula, which was flexible and responsive depending on internal and external stimulation [79]; therefore, the habenula failed to regulate startle response. MK-801-impaired habenula response was found to be hyperactive. Hypoactivation of the lateral habenula at an idle state has also been reported in MK-801-induced rats that exhibit schizophrenia-related negative and cognitive symptoms [24]. Although the NMDA receptor disruption in the habenula is not the sole contributor to the habituation impairment, the NMDA receptor plays a direct role in mediating the zebrafish locomotor circuit [47, 54]. Hence, the depolarization of Mauthner neurons by solenoid stimuli could be involved in the MK-801-induced startle habituation impairment.

Previous brain-wide imaging has shown the activation of the habenula in the startle behavioral transition from non-habituating to habituating based on the level of threat of startle stimuli in larval zebrafish [14–16]. In zebrafish, the ventral habenula has been shown to supply glutamatergic excitatory signals to the median raphe nucleus in regulating aversive learning [80]. Furthermore, serotonergic signals from the median raphe nucleus project to Mauthner neurons of the acoustic startle circuit [77]. Startle stimuli and aversive stimuli share similar commonalities in terms of the threat towards the survival of the zebrafish as the nature of startle stimuli is first perceived to be threatening before learning the neutral nature (habituated). This suggests an upstream action from the habenula-median raphe nucleus pathway to Mauthner neurons could be involved in regulating the Mauthner neurons-dependent startle habituation.

GPR139, exclusively expressed in the ventral habenula in adult zebrafish [34], has emerged as a potential regulator of startle habituation even in the larval stage. The larvae habenula were well developed and homologous to mammals as early as 4 dpf and had molecular identities similar to that of 1-year adult zebrafish [13, 81]. This complex development at the larval stage established the capability of larval zebrafish to perform various cognitive functions including startle habituation [82]. We found that

GPR139 agonists did not strongly alter the habenula spontaneous activity, while the effect of GPR139 agonists became obvious when the larvae received startle stimulation. We found exposure to GPR139 agonists elevated the habenula activities, and more neural activation was found in the ventral habenula at the end of the habituation paradigm. While habituated larvae would have elevated habenula subnuclei activity [15], the presence of GPR139 agonists further elevated the intensity of neural activation in the habenula. In addition, the locomotion test ruled out the effect of GPR139 agonists on locomotion as a confound on the startle response. The exponential decay curve fitting analysis showed that GPR139 agonists enhanced startle habituation only at the lowest concentration. Larvae treated with 20 μM and 50 μM of both JNJ-63533054 showed a delay in habituation, which was evident from the higher tau values than the control across blocks. As for TAK-041, although the tau values of 20 μM and 50 μM were similar to the control, the fluctuation in amplitude (for 20 μM) and plateau (for 50 μM) showed deviation from the normal habituation characteristics. On the contrary, for the lowest concentration of both GPR139 agonists, the plateau showed a lower habituation asymptote than the control across blocks, indicating decreased probability of startle response in the habituated condition. Also, the tau, which indicated the number of trials required to achieve habituation, of both GPR139 agonists was also lower than the control. Startle habituation is conserved across species, and since the habituation asymptote does not have a finite baseline [57], the larvae treated with the lowest concentration of both GPR139 agonists showed enhanced habituation. Hence, paired with behavioral experiment findings, activation of GPR139 signaling could lead to the activation of habenula that facilitated the enhancement of startle habituation.

On the other hand, when the larvae modeled with startle habituation impairment via MK-801, we found GPR139 agonists reversed the disrupted startle habituation and preserved the characteristics of startle habituation of the MK-801-induced larvae, suggesting that the activation of GPR139 signaling in the habenula could ameliorate the habituation capability. We found that only the lowest concentration of both MKJNJ and MKTAK groups showed a consistent decrement in amplitude, tau, and plateau across blocks compared to the fluctuating change in other concentrations and maintained lower values than the MK group. The MK-801-induced hyperactivation in the overall habenula was reduced with the treatment of GPR139 agonists at the habituated state, reversing startle habituation impairment. Co-treatment of MK-801 with either GPR139 agonists showed higher activation in the ventral habenula than the respective MK group, suggesting a greater activation in the ventral habenula while the reversal of impairment occurred. Therefore, there is a possible interactive mechanism between GPR139 and the NMDA receptor in regulating startle habituation. Though there is limited study on the interaction between GPR139 and glutaminergic signaling, sharing the site of expression in habenula and mediation in cognitive function may speculate a potential interaction as GPR139 is expressed in the glutaminergic-dominant neurons of habenula [83, 84]. Moreover, GPR139 and NMDA receptors also exhibited similar downstream $G_{q/11}$ signals in mediating fear-related cognitive functions [85, 86]. However, the current study is limited in its ability to deduce the possible mechanism between GPR139 and NMDA receptors. Future experiments will be required to directly assess the role of GPR139 on NMDA receptors during the engagement of cognitive functions.

We also noticed a difference in the effect of JNJ-63533054 and TAK-041 on the startle habituation and habenula activity of larval zebrafish. Although JNJ-63533054 and TAK-041 shared similar binding sites, the binding pockets of the structures of both agonists are distinctive, indicating the difference in activating GPR139 [40]. G protein signaling and internalization assays showed JNJ-63533054 having higher potency than TAK-041 [87]. The structure and potency difference between GPR139 agonists in the capability to activate GPR139 may directly influence habenula activity and behavioral performance.

We acknowledge the limitations of this study. Firstly, the effect of GPR139 agonists on cognitive performance could be more precisely controlled. Although we had ruled out the confound that GPR139 agonists did not influence zebrafish locomotion, the activation of GPR139 in the ventral habenula of larval zebrafish could be affected by other factors, such as the endogenous GPR139 ligands in the zebrafish central nervous system and other neuromodulator connections. The precise mechanism underlying GPR139 agonists-induced changes can be elucidated using knockout models [29]. By silencing GPR139 receptors, the effect of GPR139 agonists on behavioral and physiological zebrafish can be studied and contrasted with existing data. Moreover, since we showed a relationship between the GPR139 agonists and MK-801 on startle habituation performance, testing the GPR139 agonists on NMDA receptor knockout zebrafish may also reveal the relationship between GPR139 and the NMDA receptor in regulating cognitive performance. Hence, knockout models and other non-genetic controls, such as optogenetics, shall be explored to extend the current experiment that provided the first-step evidence on the potential of GPR139 agonists in reversing startle habituation deficits in larval zebrafish.

Secondly, in the present study, JNJ-63533054 and TAK-041, synthetic agonists for human GPR139 were adopted for zebrafish. Our previous study demonstrated JNJ-63533054 has a higher potency (3.3 folds) against zebrafish GPR139 as compared to human GPR139 [34]. However, we did not test the agonistic property of TAK-041 on zebrafish GPR139. It could be that TAK-041 had higher efficacy than JNJ-63533054 on the zebrafish model, as our experiment showed that TAK-041 could better enhance startle habituation and cause a lesser delay at 50 μM. The opposite possibility was observed in human and mouse cell cultures, in which both agonists were found to be compatible, and JNJ-63533054 showed higher efficacy compared to TAK-041 in various pharmacological assays [87]. Future experiments should compare the pharmacokinetic profile of TAK-041 and JNJ-63533054 on zebrafish to provide a pharmacological explanation of cognitive performance.

Moving forward, we aim to accumulate the evidence of GPR139 agonists on startle zebrafish habituation by examining the washout and reversibility of the agonists on zebrafish. Moreover, we aim to elucidate the relationship of GPR139 signaling with neurotransmitter systems within the habenular pathway. This will further strengthen the evidence of GPR139 in cognitive functions and the neuromodulator dysfunction related to schizophrenia in the larval zebrafish model.

We showed that GPR139 agonists, JNJ-63533054 and TAK-041, reverse and enhance MK-801-induced startle habituation impairment in larval zebrafish. While 20 μM and 50 μM of GPR139 agonists altered the characteristics of startle habituation from the standard, lower concentrations enhanced the startle habituation and reversed the MK-801-induced hyperactivity in habenula subnuclei during the habituation paradigm. Our study offered valuable insights into how the activation of GPR139 signaling can reverse startle habituation deficits in a larval zebrafish model. Additionally, we elucaited the activities of habenula subnuclei, which contributes to our understanding of the pathology of schizophrenia and cognitive function impairments.

Author Contributions

Teck Fong Kow: designed experiment, conducted the experiment and collected data, analyzed data, wrote, reviewed, and edited manuscript. Siew Ying Mok: advised experiment design and reviewed manuscript. Pek Yee Tang: reviewed manuscript. Lor Huai Chong: reviewed manuscript. Satoshi Ogawa: designed experiment, edited and reviewed manuscript.

Acknowledgments

We thank Dr. Suresh Jeyaraj Jesuthasan, Nanyang Technological University, for his guidance on suite2p software and larval zebrafish mounting preparation for in vivo calcium imaging. Open access publishing facilitated by Monash University, as part of the Wiley - Monash University agreement via the Council of Australian University Librarians.

Conflicts of Interest

The authors declare no conflicts of interest.

Data Availability Statement

Available upon request.

References

1. M. A. Geyer and G. Gross, eds., *Novel Antischizophrenia Treatments (213)* (Springer Berlin Heidelberg, 2012), https://doi.org/10.1007/978-3-642-25758-2.

2. R. O'Carroll, "Cognitive Impairment in Schizophrenia," *Advances in Psychiatric Treatment* 6, no. 3 (2000): 161–168, https://doi.org/10.1192/apt.6.3.161.

3. A. McCleery and K. H. Nuechterlein, "Cognitive Impairment in Psychotic Illness: Prevalence, Profile of Impairment, Developmental Course, and Treatment Considerations," *Dialogues in Clinical Neuroscience* 21, no. 3 (2019): 239–248, https://doi.org/10.31887/DCNS.2019.21.3/amccleery.

4. M. J. Minzenberg and C. S. Carter, "Developing Treatments for Impaired Cognition in Schizophrenia," *Trends in Cognitive Sciences* 16, no. 1 (2012): 35–42, https://doi.org/10.1016/j.tics.2011.11.017.

5. D. R. Weinberger, M. F. Egan, A. Bertolino, et al., "Prefrontal Neurons and the Genetics of Schizophrenia," *Biological Psychiatry* 50, no. 11 (2001): 825–844, https://doi.org/10.1016/S0006-3223(01)01252-5.

6. R. A. McCutcheon, R. S. E. Keefe, and P. K. McGuire, "Cognitive Impairment in Schizophrenia: Aetiology, Pathophysiology, and Treatment," *Molecular Psychiatry* 28, no. 5 (2023): 1902–1918, https://doi.org/10.1038/s41380-023-01949-9.

7. O. Hikosaka, "The Habenula: From Stress Evasion to Value-Based Decision-Making," *Nature Reviews Neuroscience* 11, no. 7 (2010): 503–513, https://doi.org/10.1038/nrn2866.

8. T. C. Jhou, H. L. Fields, M. G. Baxter, C. B. Saper, and P. C. Holland, "The Rostromedial Tegmental Nucleus (RMTg), a GABAergic Afferent to Midbrain Dopamine Neurons, Encodes Aversive Stimuli and Inhibits Motor Responses," *Neuron* 61, no. 5 (2009): 786–800, https://doi.org/10.1016/j.neuron.2009.02.001.

9. H. Ji and P. D. Shepard, "Lateral Habenula Stimulation Inhibits Rat Midbrain Dopamine Neurons Through a GABAA Receptor-Mediated Mechanism," *Journal of Neuroscience* 27, no. 26 (2007): 6923–6930, https://doi.org/10.1523/JNEUROSCI.0958-07.2007.

10. G. Ferraro, M. E. Montalbano, P. Sardo, and V. La Grutta, "Lateral Habenula and Hippocampus: A Complex Interaction Raphe Cells-Mediated," *Journal of Neural Transmission* 104, no. 6–7 (1997): 615–631, https://doi.org/10.1007/BF01291880.

11. R. Y. Wang and G. K. Aghajanian, "Inhibition of Neurons in the Amygdala by Dorsal Raphe Stimulation: Mediation Through a Direct Serotonergic Pathway," *Brain Research* 120, no. 1 (1977): 85–102, https://doi.org/10.1016/0006-8993(77)90499-1.

12. M. Agetsuma, H. Aizawa, T. Aoki, et al., "The Habenula Is Crucial for Experience-Dependent Modification of Fear Responses in Zebrafish," *Nature Neuroscience* 13, no. 11 (2010): 1354–1356, https://doi.org/10.1038/nn.2654.

13. R. Amo, H. Aizawa, M. Takahoko, et al., "Identification of the Zebrafish Ventral Habenula as a Homolog of the Mammalian Lateral Habenula," *Journal of Neuroscience* 30, no. 4 (2010): 1566–1574, https://doi.org/10.1523/JNEUROSCI.3690-09.2010.

14. H. Fotowat and F. Engert, "Neural Circuits Underlying Habituation of Visually Evoked Escape Behaviors in Larval Zebrafish," *eLife* 12 (2023): e82916, https://doi.org/10.7554/eLife.82916.

15. E. Marquez-Legorreta, L. Constantin, M. Piber, et al., "Brain-Wide Visual Habituation Networks in Wild Type and fmr1 Zebrafish," *Nature Communications* 13, no. 1 (2022), https://doi.org/10.1038/s41467-022-28299-4.

16. C. Pantoja, J. Larsch, E. Laurell, G. Marquart, M. Kunst, and H. Baier, "Rapid Effects of Selection on Brain-Wide Activity and Behavior," *Current Biology* 30, no. 18 (2020): 3647–3656.e3, https://doi.org/10.1016/j.cub.2020.06.086.

17. Y. Abuduaini, Y. Pu, P. M. Thompson, and X. Kong, "Significant Heterogeneity in Structural Asymmetry of the Habenula in the Human Brain: A Systematic Review and Meta-Analysis," *Human Brain Mapping* 44, no. 10 (2023): 4165–4182, https://doi.org/10.1002/hbm.26337.

18. H.-G. Bernstein, J. Hildebrandt, H. Dobrowolny, J. Steiner, B. Bogerts, and J. Pahnke, "Morphometric Analysis of the Cerebral Expression of ATP-Binding Cassette Transporter Protein ABCB1 in Chronic Schizophrenia: Circumscribed Deficits in the Habenula," *Schizophrenia Research* 177, no. 1–3 (2016): 52–58, https://doi.org/10.1016/j.schres.2016.02.036.

19. R. Sandyk, "Pineal and Habenula Calcification in Schizophrenia," *International Journal of Neuroscience* 67, no. 1–4 (1992): 19–30, https://doi.org/10.3109/00207459208994773.

20. K. Xue, J. Chen, Y. Wei, et al., "Altered Static and Dynamic Functional Connectivity of Habenula in First-Episode, Drug-naïve Schizophrenia Patients, and Their Association With Symptoms Including Hallucination and Anxiety," *Frontiers in Psychiatry* 14 (2023): 1078779, https://doi.org/10.3389/fpsyt.2023.1078779.

21. L. Zhang, H. Wang, S. Luan, et al., "Altered Volume and Functional Connectivity of the Habenula in Schizophrenia," *Frontiers in Human Neuroscience* 11 (2017): 636, https://doi.org/10.3389/fnhum.2017.00636.

22. S. A. Heldt and K. J. Ressler, "Lesions of the Habenula Produce Stress- and Dopamine-Dependent Alterations in Prepulse Inhibition

and Locomotion," *Brain Research* 1073 (2006): 229–239, https://doi.org/10.1016/j.brainres.2005.12.053.

23. J. A. Larrauri, D. A. Burke, B. J. Hall, and E. D. Levin, "Role of Nicotinic Receptors in the Lateral Habenula in the Attenuation of Amphetamine-Induced Prepulse Inhibition Deficits of the Acoustic Startle Response in Rats," *Psychopharmacology* 232, no. 16 (2015): 3009–3017, https://doi.org/10.1007/s00213-015-3940-z.

24. J. Li, S. Yang, X. Liu, et al., "Hypoactivity of the Lateral Habenula Contributes to Negative Symptoms and Cognitive Dysfunction of Schizophrenia in Rats," *Experimental Neurology* 318 (2019): 165–173, https://doi.org/10.1016/j.expneurol.2019.05.005.

25. L. R. Watkins and C. Orlandi, "Orphan G Protein Coupled Receptors in Affective Disorders," *Genes* 11, no. 6 (2020): 694, https://doi.org/10.3390/genes11060694.

26. C. A. Castellani, Z. Awamleh, M. G. Melka, R. L. O'Reilly, and S. M. Singh, "Copy Number Variation Distribution in Six Monozygotic Twin Pairs Discordant for Schizophrenia," *Twin Research and Human Genetics* 17, no. 2 (2014): 108–120, https://doi.org/10.1017/thg.2014.6.

27. J. L. Ebejer, D. L. Duffy, J. Van Der Werf, et al., "Genome-Wide Association Study of Inattention and Hyperactivity–Impulsivity Measured as Quantitative Traits," *Twin Research and Human Genetics* 16, no. 2 (2013): 560–574, https://doi.org/10.1017/thg.2013.12.

28. D. E. I. Gloriam, H. B. Schiöth, and R. Fredriksson, "Nine New Human Rhodopsin Family G-Protein Coupled Receptors: Identification, Sequence Characterisation and Evolutionary Relationship," *Biochimica et Biophysica Acta (BBA) – General Subjects* 1722, no. 3 (2005): 235–246, https://doi.org/10.1016/j.bbagen.2004.12.001.

29. M. Dao, H. M. Stoveken, Y. Cao, and K. A. Martemyanov, "The Role of Orphan Receptor GPR139 in Neuropsychiatric Behavior," *Neuropsychopharmacology* 47, no. 4 (2022): 902–913, https://doi.org/10.1038/s41386-021-00962-2.

30. J. Mao, Y. Cui, H. Wang, et al., "Design and Synthesis of Novel GPR139 Agonists With Therapeutic Effects in Mouse Models of Social Interaction and Cognitive Impairment," *Journal of Medicinal Chemistry* 66, no. 20 (2023): 14011–14028, https://doi.org/10.1021/acs.jmedchem.3c01034.

31. R. Mu, X. Hou, Q. Liu, W. Wang, C. Qin, and H. Li, "Up-Regulation of GPR139 in the Medial Septum Ameliorates Cognitive Impairment in Two Mouse Models of Alzheimer's Disease," *International Immunopharmacology* 130 (2024): 111786, https://doi.org/10.1016/j.intimp.2024.111786.

32. P. A. S. Nogueira, A. Moura-Assis, A. M. Zanesco, et al., "The Orphan G Protein-Coupled Receptor, GPR139, Is Expressed in the Hypothalamus and Is Involved in the Regulation of Body Mass, Blood Glucose, and Insulin," *Neuroscience Letters* 792 (2023): 136955, https://doi.org/10.1016/j.neulet.2022.136955.

33. U. Süsens, I. Hermans-Borgmeyer, J. Urny, and H. C. Schaller, "Characterisation and Differential Expression of Two Very Closely Related G-Protein-Coupled Receptors, GPR139 and GPR142, in Mouse Tissue and During Mouse Development," *Neuropharmacology* 50, no. 4 (2006): 512–520, https://doi.org/10.1016/j.neuropharm.2005.11.003.

34. N. Roy, S. Ogawa, R. Maniam, and I. Parhar, "Habenula GPR139 Is Associated With Fear Learning in the Zebrafish," *Scientific Reports* 11, no. 1 (2021): 5549, https://doi.org/10.1038/s41598-021-85002-1.

35. C. A. Dvorak, H. Coate, D. Nepomuceno, et al., "Identification and SAR of Glycine Benzamides as Potent Agonists for the GPR139 Receptor," *ACS Medicinal Chemistry Letters* 6, no. 9 (2015): 1015–1018, https://doi.org/10.1021/acsmedchemlett.5b00247.

36. V. Isberg, K. B. Andersen, C. Bisig, G. P. H. Dietz, H. Bräuner-Osborne, and D. E. Gloriam, "Computer-Aided Discovery of Aromatic l -α-Amino Acids as Agonists of the Orphan G Protein-Coupled Receptor GPR139," *Journal of Chemical Information and Modeling* 54, no. 6 (2014): 1553–1557, https://doi.org/10.1021/ci500197a.

37. C. Liu, P. Bonaventure, G. Lee, et al., "GPR139, an Orphan Receptor Highly Enriched in the Habenula and Septum, Is Activated by the Essential Amino Acids l-Tryptophan and l-Phenylalanine," *Molecular Pharmacology* 88, no. 5 (2015): 911–925, https://doi.org/10.1124/mol.115.100412.

38. A. C. Nøhr, M. A. Shehata, A. S. Hauser, et al., "The Orphan G Protein-Coupled Receptor GPR139 Is Activated by the Peptides: Adrenocorticotropic Hormone (ACTH), α-, and β-Melanocyte Stimulating Hormone (α-MSH, and β-MSH), and the Conserved Core Motif HFRW," *Neurochemistry International* 102 (2017): 105–113, https://doi.org/10.1016/j.neuint.2016.11.012.

39. L. Vedel, A. C. Nøhr, D. E. Gloriam, and H. Bräuner-Osborne, "Pharmacology and Function of the Orphan GPR139 G Protein-Coupled Receptor," *Basic & Clinical Pharmacology & Toxicology* 126, no. S6 (2020): 35–46, https://doi.org/10.1111/bcpt.13263.

40. Y. Zhou, H. Daver, B. Trapkov, et al., "Molecular Insights Into Ligand Recognition and G Protein Coupling of the Neuromodulatory Orphan Receptor GPR139," *Cell Research* 32, no. 2 (2022): 210–213, https://doi.org/10.1038/s41422-021-00591-w.

41. H. A. Reichard, H. H. Schiffer, H. Monenschein, et al., "Discovery of TAK-041: A Potent and Selective GPR139 Agonist Explored for the Treatment of Negative Symptoms Associated With Schizophrenia," *Journal of Medicinal Chemistry* 64, no. 15 (2021): 11527–11542, https://doi.org/10.1021/acs.jmedchem.1c00820.

42. J. Kononoff, M. Kallupi, A. Kimbrough, D. Conlisk, G. De Guglielmo, and O. George, "Systemic and Intra-Habenular Activation of the Orphan G Protein-Coupled Receptor GPR139 Decreases Compulsive-Like Alcohol Drinking and Hyperalgesia in Alcohol-Dependent Rats," *Eneuro* 5, no. 3 (2018): ENEURO.0153-18.2018, https://doi.org/10.1523/ENEURO.0153-18.2018.

43. L. Wang, C. Dugovic, S. Yun, et al., "Putative Role of GPR139 on Sleep Modulation Using Pharmacological and Genetic Rodent Models," *European Journal of Pharmacology* 882 (2020): 173256, https://doi.org/10.1016/j.ejphar.2020.173256.

44. C. J. Hatzipantelis, M. Langiu, T. H. Vandekolk, et al., "Translation-Focused Approaches to GPCR Drug Discovery for Cognitive Impairments Associated With Schizophrenia," *ACS Pharmacology & Translational Science* 3, no. 6 (2020): 1042–1062, https://doi.org/10.1021/acsptsci.0c00117.

45. W. Yin, D. Han, P. Khudyakov, et al., "A Phase 1 Study to Evaluate the Safety, Tolerability and Pharmacokinetics of TAK-041 in Healthy Participants and Patients With Stable Schizophrenia," *British Journal of Clinical Pharmacology* 88, no. 8 (2022): 3872–3882, https://doi.org/10.1111/bcp.15305.

46. M. Christou, A. Kavaliauskis, E. Ropstad, and T. W. K. Fraser, "DMSO Effects Larval Zebrafish (*Danio rerio*) Behavior, With Additive and Interaction Effects When Combined With Positive Controls," *Science of the Total Environment* 709 (2020): 134490, https://doi.org/10.1016/j.scitotenv.2019.134490.

47. A. C. Roberts, J. Reichl, M. Y. Song, et al., "Habituation of the C-Start Response in Larval Zebrafish Exhibits Several Distinct Phases and Sensitivity to NMDA Receptor Blockade," *PLoS One* 6, no. 12 (2011): e29132, https://doi.org/10.1371/journal.pone.0029132.

48. M. A. Wolman, R. A. Jain, L. Liss, and M. Granato, "Chemical Modulation of Memory Formation in Larval Zebrafish," *Proceedings of the National Academy of Sciences* 108, no. 37 (2011): 15468–15473, https://doi.org/10.1073/pnas.1107156108.

49. K. Gawel, N. S. Banono, A. Michalak, and C. V. Esguerra, "A Critical Review of Zebrafish Schizophrenia Models: Time for Validation?," *Neuroscience & Biobehavioral Reviews* 107 (2019): 6–22, https://doi.org/10.1016/j.neubiorev.2019.08.001.

50. J. J. Ingebretson and M. A. Masino, "Quantification of Locomotor Activity in Larval Zebrafish: Considerations for the Design of

High-Throughput Behavioral Studies," *Frontiers in Neural Circuits* 7 (2013), https://doi.org/10.3389/fncir.2013.00109.

51. H. A. Burgess and M. Granato, "Modulation of Locomotor Activity in Larval Zebrafish During Light Adaptation," *Journal of Experimental Biology* 210, no. 14 (2007): 2526–2539, https://doi.org/10.1242/jeb.003939.

52. S. Padilla, D. L. Hunter, B. Padnos, S. Frady, and R. C. MacPhail, "Assessing Locomotor Activity in Larval Zebrafish: Influence of Extrinsic and Intrinsic Variables," *Neurotoxicology and Teratology* 33, no. 6 (2011): 624–630, https://doi.org/10.1016/j.ntt.2011.08.005.

53. M. U. Tuz-Sasik, H. Boije, and R. Manuel, "Characterization of Locomotor Phenotypes in Zebrafish Larvae Requires Testing Under Both Light and Dark Conditions," *PLoS One* 17, no. 4 (2022): e0266491, https://doi.org/10.1371/journal.pone.0266491.

54. J. D. Best, S. Berghmans, J. J. F. G. Hunt, et al., "Non-Associative Learning in Larval Zebrafish," *Neuropsychopharmacology* 33, no. 5 (2008): 1206–1215, https://doi.org/10.1038/sj.npp.1301489.

55. R. M. Colwill and R. Creton, "Imaging Escape and Avoidance Behavior in Zebrafish Larvae," *Reviews in the Neurosciences* 22, no. 1 (2011): 63–73, https://doi.org/10.1515/RNS.2011.008.

56. M. A. Geyer, N. R. Swerdlow, R. S. Mansbach, and D. L. Braff, "Startle Response Models of Sensorimotor Gating and Habituation Deficits in Schizophrenia," *Brain Research Bulletin* 25, no. 3 (1990): 485–498, https://doi.org/10.1016/0361-9230(90)90241-Q.

57. C. H. Rankin, T. Abrams, R. J. Barry, et al., "Habituation Revisited: An Updated and Revised Description of the Behavioral Characteristics of Habituation," *Neurobiology of Learning and Memory* 92, no. 2 (2009): 135–138, https://doi.org/10.1016/j.nlm.2008.09.012.

58. E. L. Troconis, A. J. Ordoobadi, T. F. Sommers, R. Aziz-Bose, A. R. Carter, and J. G. Trapani, "Intensity-Dependent Timing and Precision of Startle Response Latency in Larval Zebrafish," *Journal of Physiology* 595, no. 1 (2017): 265–282, https://doi.org/10.1113/JP272466.

59. W.-Y. Png, P.-Y. Tang, S. Ogawa, I. Parhar, and S.-Y. Mok, "Startle Habituation: A Tool for Assessing Information Processing Deficits in Zebrafish Model of Schizophrenia," *Sains Malaysiana* 50, no. 1 (2021): 201–206, https://doi.org/10.17576/jsm-2021-5001-20.

60. S. Banerjee, L. E. Ranspach, X. Luo, et al., "Vision and Sensorimotor Defects Associated With Loss of Vps11 Function in a Zebrafish Model of Genetic Leukoencephalopathy," *Scientific Reports* 12, no. 1 (2022): 3511, https://doi.org/10.1038/s41598-022-07448-1.

61. C. Beppi, D. Straumann, and S. Y. Bögli, "A Model-Based Quantification of Startle Reflex Habituation in Larval Zebrafish," *Scientific Reports* 11, no. 1 (2021): 846, https://doi.org/10.1038/s41598-020-79923-6.

62. M. Kunst, E. Laurell, N. Mokayes, et al., "A Cellular-Resolution Atlas of the Larval Zebrafish Brain," *Neuron* 103, no. 1 (2019): 21–38.e5, https://doi.org/10.1016/j.neuron.2019.04.034.

63. I. Shainer, E. Kuehn, E. Laurell, et al., "A Single-Cell Resolution Gene Expression Atlas of the Larval Zebrafish Brain," *Science Advances* 9, no. 8 (2023): eade9909, https://doi.org/10.1126/sciadv.ade9909.

64. C. A. Schneider, W. S. Rasband, and K. W. Eliceiri, "NIH Image to ImageJ: 25 Years of Image Analysis," *Nature Methods* 9, no. 7 (2012): 671–675, https://doi.org/10.1038/nmeth.2089.

65. M. Pachitariu, C. Stringer, M. Dipoppa, et al., "Suite2p: Beyond 10,000 Neurons With Standard Two-Photon Microscopy," (2016), *bioRxiv*, https://doi.org/10.1101/061507.

66. L. Avitan, Z. Pujic, J. Mölter, et al., "Spontaneous Activity in the Zebrafish Tectum Reorganizes Over Development and Is Influenced by Visual Experience," *Current Biology* 27, no. 16 (2017): 2407–2419.e4, https://doi.org/10.1016/j.cub.2017.06.056.

67. S. Fore, F. Acuña-Hinrichsen, K. A. Mutlu, et al., "Functional Properties of Habenular Neurons Are Determined by Developmental Stage and Sequential Neurogenesis," *Science Advances* 6, no. 36 (2020): eaaz3173, https://doi.org/10.1126/sciadv.aaz3173.

68. L. Corradi, M. Zaupa, S. Sawamiphak, and A. Filosa, "Using pERK Immunostaining to Quantify Neuronal Activity Induced by Stress in Zebrafish Larvae," *STAR Protocols* 3, no. 4 (2022): 101731, https://doi.org/10.1016/j.xpro.2022.101731.

69. D. Klamer, E. Pålsson, A. Revesz, J. A. Engel, and L. Svensson, "Habituation of Acoustic Startle Is Disrupted by Psychotomimetic Drugs: Differential Dependence on Dopaminergic and Nitric Oxide Modulatory Mechanisms," *Psychopharmacology* 176, no. 3–4 (2004): 440–450, https://doi.org/10.1007/s00213-004-1901-z.

70. K. C. Marsden and M. Granato, "In Vivo Ca2+ Imaging Reveals That Decreased Dendritic Excitability Drives Startle Habituation," *Cell Reports* 13, no. 9 (2015): 1733–1740, https://doi.org/10.1016/j.celrep.2015.10.060.

71. J. H. Wang, J. Short, C. Ledent, A. J. Lawrence, and M. V. D. Buuse, "Reduced Startle Habituation and Prepulse Inhibition in Mice Lacking the Adenosine A2A Receptor," *Behavioural Brain Research* 143, no. 2 (2003): 201–207, https://doi.org/10.1016/S0166-4328(03)00036-6.

72. V. Lopes-dos-Santos, S. Ribeiro, and A. B. L. Tort, "Detecting Cell Assemblies in Large Neuronal Populations," *Journal of Neuroscience Methods* 220, no. 2 (2013): 149–166, https://doi.org/10.1016/j.jneumeth.2013.04.010.

73. J. S. Yeomans and P. W. Frankland, "The Acoustic Startle Reflex: Neurons and Connections," *Brain Research Reviews* 21, no. 3 (1995): 301–314, https://doi.org/10.1016/0165-0173(96)00004-5.

74. K. Fero, T. Yokogawa, and H. A. Burgess, "The Behavioral Repertoire of Larval Zebrafish," in *Zebrafish Models in Neurobehavioral Research*, vol. 52, ed. A. V. Kalueff and J. M. Cachat (Humana Press, 2011), 249–291, https://doi.org/10.1007/978-1-60761-922-2_12.

75. H. A. Burgess and M. Granato, "Sensorimotor Gating in Larval Zebrafish," *Journal of Neuroscience* 27, no. 18 (2007): 4984–4994, https://doi.org/10.1523/JNEUROSCI.0615-07.2007.

76. J. R. Fetcho and K. S. Liu, "Zebrafish as a Model System for Studying Neuronal Circuits and Behavior a," *Annals of the New York Academy of Sciences* 860, no. 1 (1998): 333–345, https://doi.org/10.1111/j.1749-6632.1998.tb09060.x.

77. C. Pantoja, A. Hoagland, E. C. Carroll, V. Karalis, A. Conner, and E. Y. Isacoff, "Neuromodulatory Regulation of Behavioral Individuality in Zebrafish," *Neuron* 91, no. 3 (2016): 587–601, https://doi.org/10.1016/j.neuron.2016.06.016.

78. A. C. Roberts, K. C. Pearce, R. C. Choe, et al., "Long-Term Habituation of the C-Start Escape Response in Zebrafish Larvae," *Neurobiology of Learning and Memory* 134 (2016): 360–368, https://doi.org/10.1016/j.nlm.2016.08.014.

79. Suryadi, R.-K. Cheng, E. Birkett, S. Jesuthasan, and L. Y. Chew, "Dynamics and Potential Significance of Spontaneous Activity in the Habenula," *Eneuro* 9, no. 5 (2022): 2022, https://doi.org/10.1523/ENEURO.0287-21.2022.

80. R. Amo, F. Fredes, M. Kinoshita, et al., "The Habenulo-Raphe Serotonergic Circuit Encodes an Aversive Expectation Value Essential for Adaptive Active Avoidance of Danger," *Neuron* 84, no. 5 (2014): 1034–1048, https://doi.org/10.1016/j.neuron.2014.10.035.

81. S. Pandey, K. Shekhar, A. Regev, and A. F. Schier, "Comprehensive Identification and Spatial Mapping of Habenular Neuronal Types Using Single-Cell RNA-Seq," *Current Biology* 28, no. 7 (2018): 1052–1065.e7, https://doi.org/10.1016/j.cub.2018.02.040.

82. M. Wolman and M. Granato, "Behavioral Genetics in Larval Zebrafish: Learning From the Young," *Developmental Neurobiology* 72, no. 3 (2012): 366–372, https://doi.org/10.1002/dneu.20872.

83. M. Blank, L. D. Guerim, R. F. Cordeiro, and M. R. M. Vianna, "A One-Trial Inhibitory Avoidance Task to Zebrafish: Rapid Acquisition of

an NMDA-Dependent Long-Term Memory," *Neurobiology of Learning and Memory* 92, no. 4 (2009): 529–534, https://doi.org/10.1016/j.nlm.2009.07.001.

84. M.-C. Ng, C.-P. Hsu, Y.-J. Wu, S.-Y. Wu, Y.-L. Yang, and K.-T. Lu, "Effect of MK-801-Induced Impairment of Inhibitory Avoidance Learning in Zebrafish via Inactivation of Extracellular Signal-Regulated Kinase (ERK) in Telencephalon," *Fish Physiology and Biochemistry* 38, no. 4 (2012): 1099–1106, https://doi.org/10.1007/s10695-011-9595-8.

85. A. McEwan, *Modulation of Habituation Kinetics and Behavioural Shifts by Members of the Heterotrimeric G-Protein Signaling Pathways (T)* (University of British Columbia, 2013), https://open.library.ubc.ca/collections/ubctheses/24/items/1.0073828.

86. D. Peterlik, P. J. Flor, and N. Uschold-Schmidt, "The Emerging Role of Metabotropic Glutamate Receptors in the Pathophysiology of Chronic Stress-Related Disorders," *Current Neuropharmacology* 14, no. 5 (2016): 514–539, https://doi.org/10.2174/1570159x13666150515234920.

87. L. Pallareti, T. F. Rath, B. Trapkov, et al., "Pharmacological Characterization of Novel Small Molecule Agonists and Antagonists for the Orphan Receptor GPR139," *European Journal of Pharmacology* 943 (2023): 175553, https://doi.org/10.1016/j.ejphar.2023.175553.

Supporting Information

Additional supporting information can be found online in the Supporting Information section.